RNA Helicases From the DEA(D/H)-box Family Contribute to Plant NMD Efficiency

Aleksandra Sulkowska, Andor Auber, Pawel Sikorski, Dániel Silhavy, Mariann Auth, Ewa Sitkiewicz, Viviane Jean, Rémy Merret, Cécile Bousquet-Antonelli, Joanna Kufel

▶ **To cite this version:**

Aleksandra Sulkowska, Andor Auber, Pawel Sikorski, Dániel Silhavy, Mariann Auth, et al.. RNA Helicases From the DEA(D/H)-box Family Contribute to Plant NMD Efficiency. Plant and Cell Physiology, In press, 10.1093/pcp/pcz186 . hal-02301050

HAL Id: hal-02301050
https://univ-perp.hal.science/hal-02301050

Submitted on 19 Dec 2019

HAL is a multi-disciplinary open access archive for the deposit and dissemination of scientific research documents, whether they are published or not. The documents may come from teaching and research institutions in France or abroad, or from public or private research centers.

L'archive ouverte pluridisciplinaire **HAL**, est destinée au dépôt et à la diffusion de documents scientifiques de niveau recherche, publiés ou non, émanant des établissements d'enseignement et de recherche français ou étrangers, des laboratoires publics ou privés.

OXFORD UNIVERSITY PRESS | Plant and Cell Physiology

RNA Helicases From the DEA(D/H)-box Family Contribute to Plant NMD Efficiency

Journal:	*Plant and Cell Physiology*
Manuscript ID	PCP-2019-E-00164.R2
Manuscript Type:	Regular Paper
Date Submitted by the Author:	n/a
Complete List of Authors:	Sulkowska, Aleksandra; Warsaw University Faculty of Biology, Institute of Genetics and Biotechnology Auber, Andor; Agricultural Biotechnology Center, Agricultural Biotechnology Center Sikorski, Paweł; Warsaw University Faculty of Biology, Institute of Genetics and Biotechnology Silhavy, Dániel; Agricultural Biotechnology Center, Agricultural Biotechnology Center Auth, Mariann; Agricultural Biotechnology Center, Agricultural Biotechnology Center Sitkiewicz, Ewa; Polish Academy of Sciences Institute of Biochemistry and Biophysics, Biophysics Department, Proteomics Laboratory Jean, Viviane; Universite de Perpignan, Université de Perpignan Via Domitia Merret, Rémy; Universite de Perpignan, Université de Perpignan Via Domitia Bousquet-Antonelli, Cecile; CNRS, LGDP-UMR 5096; Kufel, Joana; Warsaw University Faculty of Biology, Institute of Genetics and Biotechnology
Keywords:	DEA(D/H)-box RNA helicases, Nonsense Mediated mRNA decay, NMD, P-bodies, RNA quality control, UPF1

SCHOLARONE™
Manuscripts

RNA Helicases From the DEA(D/H)-box Family Contribute to Plant NMD Efficiency

New plant NMD factors

Corresponding author: J. Kufel
Institute of Genetics and Biotechnology, Faculty of Biology, University of Warsaw, Pawinskiego 5a, 02-106 Warsaw, Poland
phone: +48-22-5922245; Fax: +48-22-5292244; E-mail: kufel@ibb.waw.pl

Subject areas: (3) regulation of gene expression, (4) proteins, enzymes and metabolism

Color figures: 4
Tables: 2
Supplementary material: 5 tables and 9 color figures.

For Peer Review

RNA Helicases From the DEA(D/H)-box Family Contribute to Plant NMD Efficiency

New plant NMD factors

Aleksandra Sulkowska[1], Andor Auber[2], Pawel J. Sikorski[1,†], Dániel Silhavy[2,#], Mariann Auth[2], Ewa Sitkiewicz[5], Viviane Jean[3,4],Rémy Merret[3,4], Cécile Bousquet-Antonelli[3,4] and Joanna Kufel[1*]

[1]Institute of Genetics and Biotechnology, Faculty of Biology, University of Warsaw, Pawinskiego 5a, 02-106 Warsaw, Poland

[2]Agricultural Biotechnology Center, Szent-Györgyi 4, H-2100, Gödöllő, Hungary

[3]UMR5096 LGDP, Université de Perpignan Via Domitia, UMR5096 LGDP58, Avenue Paul Alduy, 66860 Perpignan Cedex, France

[4]CNRS, UMR5096 LGDP, Perpignan Cedex, France

[5]Proteomics Laboratory, Biophysics Department, Institute of Biochemistry and Biophysics, Polish Academy of Sciences, Pawinskiego 5a, 02-106 Warszawa, Poland

[*]Corresponding author

Phone: +48-22-5922245; Fax: +48-22-5292244; E-mail:kufel@ibb.waw.pl

[†]present address - Centre of New Technologies, University of Warsaw, Banacha 2c, 02-097 Warsaw, Poland

[#]present address - Biological Research Centre, Hungarian Academy of Sciences, Institute of Plant Biology, H-6726 Szeged, Temesvári krt. 62, Hungary

For Peer Review

ABSTRACT

Nonsense-mediated mRNA decay (NMD) is a conserved eukaryotic RNA surveillance mechanism that degrades aberrant mRNAs containing a premature translation termination codon. The ATP-dependent RNA helicase Up-frameshift 1 (UPF1) is a major NMD factor in all studied organisms; however, the complexity of this mechanism has not been fully characterized in plants. To identify plant NMD factors, we analyzed UPF1-interacting proteins using tandem-affinity purification coupled to mass spectrometry. Canonical members of the NMD pathway were found along with numerous NMD candidate factors, including conserved DEA(D/H)-box RNA helicase homologs of human DDX3, DDX5 and DDX6, translation initiation factors, ribosomal proteins and transport factors. Our functional studies revealed that depletion of DDX3 helicases enhances the accumulation of NMD-target reporter mRNAs but does not result in increased protein levels. In contrast, silencing of DDX6 group leads to decreased accumulation of the NMD substrate. The inhibitory effect of DDX6-like helicases on NMD was confirmed by transient overexpression of RH12 helicase. These results indicate that DDX3 and DDX6 helicases in plants have a direct and opposing contribution to NMD and act as functional NMD factors.

Keywords

DEA(D/H)-box RNA helicases, Nonsense Mediated mRNA decay, NMD, P-bodies, RNA quality control, UPF1.

For Peer Review

INTRODUCTION

Regulation of gene expression depends on precise quality control mechanisms that regulate the balance between RNA synthesis, decay and translation. One of them, nonsense-mediated mRNA decay (NMD), is a conserved mRNA surveillance system, which besides a quality control function, regulates expression of physiological transcripts (5-30%, depending on the organism) and plays an important role in adaptation to various stresses (reviewed in Lykke-Andersen and Jensen, 2015).

NMD mainly leads to the recognition and degradation of aberrant mRNAs with premature termination codons (PTC), which is thought to prevent synthesis of potentially harmful truncated proteins. RNAs preferentially targeted by NMD also contain introns in the 3' untranslated region (UTR), exceptionally long 3'UTR or upstream open reading frames (uORFs) in the 5'UTR (reviewed in Mühlemann, 2008, Schweingruber et al. 2013, Hug et al. 2016, Karousis and Mühlemann, 2018). These features arrest the ribosome at the translation termination step, which leads to the marking of the transcript as an NMD substrate. In addition to *cis*-acting elements, NMD machinery requires highly conserved *trans*-acting core factors. The core components of the NMD pathway, UPF1, UPF2, UPF3 (also known as the suppressor with morphological effect on genitalia SMG2, SMG3 and SMG4), have been identified in yeast, nematodes, humans, flies and plants (reviewed in Raxwal and Riha, 2016). UPF1 is a central NMD effector and is an RNA helicase that interacts with UPF2 and UPF3. It is the most conserved of UPF proteins. Moreover, it plays additional roles besides NMD, including Staufen 1-mediated mRNA decay (SMD), histone mRNA decay, Tudor-SN-mediated microRNA decay, genome stability and telomere maintenance (Peccarelli and Kebaara, 2014, reviewed in Kim and Maquat, 2019).

Recognition of NMD substrates involves either the splicing- or long 3'UTR-dependent mechanisms. In mammals, a PTC present 50-55 nucleotides upstream of the exon-exon boundary detains the ribosome together with translation termination factors eRF1 and eRF3, preventing removal of the multiprotein Exon Junction Complex (EJC) that is deposited upstream from the exon-exon boundary during splicing (Nagy and Maquat 1998, Tian et al. 2017, Lloyd et al. 2018). Retention of the EJC in turn precludes interaction with Poly(A) Binding Proteins (PABPs) and contributes to the formation of the surveillance (SURF) complex with UPF1 and SMG1 kinase and the decay-inducing (DECID) complex between SURF and EJC via the UPF1-UPF2-UPF3 interaction. NMD activation requires phosphorylation of UPF1 by SMG1 kinase, resulting in binding of the remaining SMG proteins together with general mRNA decay factors, triggering mRNA degradation. A long 3'UTR-dependent mechanism (also called *faux* 3'UTR) can also occur for intronless genes, e.g. in the yeast *Saccharomyces cerevisiae.* Stalling of the ribosome on a PTC precludes the interaction of PABPs with eRF1 and eRF3, which normally facilitates translation termination at the proper stop codon and release of the newly formed polypeptide (reviewed in He

For Peer Review

and Jacobson, 2015, Karousis and Mühlemann, 2018). A more recent model proposes that degradation of PTC-containing mRNAs is triggered by a low ribosomal occupancy on long stretches of unprotected transcript (reviewed in Brogna et al. 2016, Celik et al. 2017). This model partially explains why apparently normal wild-type mRNAs are also NMD substrates and highlights an important role of active translation in the definition of correct or aberrant transcripts.

The formation of the NMD complex leads to the rapid degradation of target transcripts either by removal of the 5′ cap structure by the DCP1/DCP2 decapping complex followed by 5′→3′ exonucleolytic digestion catalyzed by the cytoplasmic exoribonuclease XRN1 or through 3′→5′ decay by the cytoplasmic exosome complex. In higher eukaryotes, degradation of NMD substrates is triggered by binding of phospho-UPF1 to SMG5:SMG7 and/or SMG5:PNRC2 (proline-rich nuclear receptor coregulatory 2 protein) and recruitment of the DCP1/DCP2 complex. In contrast, the predominant pathway in *Drosophila melanogaster*, which also operates in human cells, involves endonucleolytic cleavage by SMG6 at a position proximal to the PTC, followed by degradation of the resulting 5′ and 3′ products by the exosome and XRN1, respectively (reviewed in Nicholson and Mühlemann, 2010, Schoenberg and Maquat, 2012, He and Jacobson, 2015, Schweingruber et al. 2013). Degradation of NMD substrates occurs in the cytoplasm, most likely on mono- and polyribosomes, although previously it was proposed to take place in specific cytoplasmic structures called P-bodies (Hu et al. 2010, reviewed in Chantarachot and Bailey-Serres, 2018, Standart and Weil, 2018).

Beyond the well-described NMD core trans-acting factors, additional NMD components have been recently identified, although in most cases their exact role in this process is not well characterized (reviewed in Hug et al. 2016). Among these, the most numerous are RNA helicases (RHs) such as RUVBL1 and RUVBL2 that are required for DECID complex formation, and MOV10, which binds to RNA in a close proximity to UPF1 and is involved in the degradation of NMD substrates (Izumi et al. 2010, Gregersen et al. 2014). RNA helicases from the DEA(D/H)-box family have been shown to play an important role in different stages of NMD in human cells, *Caenorhabditis elegans* and *Danio rerio* (Longman et al. 2007, Anastasaki et al. 2011, Geißler et al. 2013, Gregersen et al. 2014). For example, human DDX5 and DDX17 bind the UPF complex and regulate the level of selected mRNAs via the NMD pathway (Geißler et al. 2013). DHX34 interacts with UPF1, UPF3, SMG1, SMG6 and SMG7 and contributes to UPF2 recruitment, UPF1 phosphorylation and the release of eRF3 from UPF1. This helicase has a strong contribution to NMD through preferential association with the SURF complex and activation of the DECID complex (Longman et al. 2007, Anastasaki et al. 2011, Longman et al. 2013, Hug and Cáceres, 2014, Melero et al. 2016). DDX6, a well-known mRNA decay cofactor and translation repressor, is a key component of P-bodies and associates with the EJC and several NMD-related complexes,

For Peer Review

including the decapping complex, the CPEB translation repression complex and the CCR4/NOT deadenylation complex (reviewed in Ostareck et al. 2014, Standart and Weil, 2018). Finally, DDX3 was recently identified as a potential interactor of UPF1, UPF2 and SMG5 (Schweingruber et al. 2016). Other proteins that interact with the NMD complex and are potentially relevant for this process in human cells include the subunits of eukaryotic initiation factor 3 (eIF3), eIF4AII, transcription-export (TREX) complex, and nucleus-associated RNA-binding proteins (Flury et al. 2014, Morris et al. 2007, Schweingruber et al. 2016).

In plants the core NMD components UPF1, UPF2 and UPF3 have been identified and their involvement in NMD demonstrated using *upf Arabidopsis thaliana* mutants or silencing of NMD factors in *Nicotiana benthamiana* and *Nicotiana attenuata* plants (Hori and Watanabe, 2005, Arciga-Reyes et al. 2006, Wu et al. 2007, Kerényi et al. 2008, reviewed in Shaul, 2015). In addition, homologs of mammalian components of the EJC complex, SMG1 and SMG7, but not of other SMG proteins or PNRC2, are present in most plants and function in NMD (Kerényi et al. 2008, Riehs et al. 2006, Riehs-Kearnan et al. 2012, Causier et al. 2017). Transient NMD assays in *Nicotiana benthamiana* combined with virus-induced gene silencing (VIGS) revealed that UPF1, UPF2 and SMG7 are involved in both long 3'UTR-based and intron-based NMD, whereas EJC components Barentsz, eIF4AIII, Y14 and Magoh are required only for intron-based NMD (Kerényi et al. 2008, Nyikó et al. 2013). Also analysis of *A. thaliana smg7* mutants confirmed its function as a major NMD factor (Riehs et al. 2006, Riehs-Kearnan et al. 2012). In turn, SMG1 kinase homolog has been identified in most plants, including *Arabidopsis lyrata* and *Physcomitrella patens*, but it is missing in *A. thaliana* (Lloyd and Davies 2013, Kerényi et al. 2013, Causier et al. 2017). Still, phosphorylation of AtUPF1 is as important as in other organisms, implying that it is probably carried out by more than one kinase (Lloyd and Davies 2013, Kerényi et al. 2013). Later steps in plant NMD, including degradation of aberrant mRNAs and non-coding RNAs, are poorly characterized. In contrast to other eukaryotes, only one additional NMD component has been described in plants, namely FIERY2 (FRY2), the RNA polymerase II C-terminal domain phosphatase-like protein that physically interacts with UPF3 and eIF4AIII and affects accumulation of NMD substrates (Cui et al. 2016).

A recently published UPF1 interactome from *A. thaliana* flowers revealed an interaction network between factors involved in NMD (UPF1, UPF3), RNA decay (decapping associated factors DCP1, DCP5 and VCS), and other aspects of RNA metabolism (DEA(D/H)-box RNA helicases from DDX3, DDX6 and DDX17 family, several PABPs) (Chicois et al. 2018). This network of known and novel P-body components and translation repression factors is consistent with the notion that also in plants P-bodies contribute to the equilibrium between RNA degradation, storage and translational repression.

For Peer Review

We have used tandem affinity purification (TAP) followed by mass spectrometry (MS) to identify UPF1-interacting proteins in 14-days-old *A. thaliana* seedlings. UPF1 interactors include known as well as new potential auxiliary plant NMD factors, such as (DEA(D/H)-box RNA helicases, splicing factors, translation initiation factors, and ribosomal and RNA binding proteins. We present functional analyses of DEA(D/H)-box RNA helicases, homologs of human DDX3 and DDX6 proteins. Subcellular localization and the analysis of reporter NMD substrates suggest that DEA(D/H)-box RNA helicases from different subfamilies have opposing regulatory effects on NMD efficiency. Arabidopsis DDX3 homologs act as NMD activators, while homologs of DDX6, a well-known component of P-bodies, have inhibitory effects on NMD.

For Peer Review

RESULTS

Identification of new UPF1-interacting proteins

To characterize the plant NMD complex we purified and identified proteins interacting with UPF1 using immunoprecipitation. We generated stable transgenic plants expressing tagged UPF1-SF (2xStrep-FLAG) in the *upf1-5* mutant. The expression of UPF1-SF protein reverted the molecular phenotypes of the *upf1-5* mutant, confirming that the fusion protein was functional (Supplementary Fig. S1). To identify proteins co-purifying with UPF1 via protein-protein and not RNA-mediated interactions, lysates prepared from the tagged line and wild-type control were treated with RNase A. Whole eluate mixtures after co-immunoprecitpitation (co-IP) were concentrated and subjected to the liquid chromatography-tandem mass spectrometry analysis (LC MS/MS). Proteins that were identified in at least two out of three UPF1 co-IP samples or enriched compared to negative controls are listed in Supplementary Table S1, whereas the most interesting proteins related to RNA metabolism and/or NMD, are summarized in Table1.

Among proteins co-purifying with UPF1-SF we identified UPF2 and UPF3, supporting the effectiveness of the NMD-complex purification. Although NMD is strictly coupled to translation termination, neither eRF1 nor eRF3 was immunoprecipitated with UPF1. We also failed to recover SMG7, even though we have previously demonstrated that SMG7 interacts with UPF1 in P-bodies in a phosphorylation-dependent manner (Kerényi et al. 2013). In recent interactome-mass spectrometry studies in human and in Arabidopsis, UPF1 did not co-purify with SMG7, indicating that the UPF1-SMG7 interaction may be labile and transient in both plant and human cells (Flury et al. 2014, Schweingruber et al. 2016, Chicois et al. 2018). Decapping factors as well as general RNA decay proteins, which in animal cells associate with the NMD complex through SMG5:SMG7 and/or SMG5:PNRC2 heterodimers (Loh et al. 2013, Cho et al. 2013, Schweingruber et al. 2016), also did not co-purify with UPF1. However, a recent study of the UPF1 interactome in plants demonstrated an RNA-dependent interaction with components of the decapping complex, indicating that UPF1 and decapping factors could be present on the same RNA substrates (Chicois et al. 2018). Comparison of the two set of UPF1-interacting proteins revealed 17 common proteins, possibly as a result of using different plant material, 14-days-old seedlings or flowers, respectively (Supplementary Table S2, Chicois et al. 2018). Still, common proteins include UPF1-3, DEA(D/H)-box RNA helicases from DDX3, DDX5 and DDX6 group, Poly(A) binding proteins (PAB2, PAB3, PAB4 and PAB8) and eIF4A. The presence of the same RNA helicases in the two sets suggests that helicases from these families may indeed represent additional NMD factors. Among other UPF1-interacting proteins were also SR34, SR34a, RS41 and SR35 alternative splicing factors (Table 1, Supplementary Table S1), supporting a direct link between these processes where in alternative splicing is a major source of PTC-containing mRNAs targeted for NMD (Drechsel et al. 2013).

For Peer Review

The set of proteins co-purifying with UPF1 also confirms a close connection of the plant NMD complex with translation initiation factors and ribosomes. We identified a representative group of ribosomal proteins (13 from the 40S subunit and 4 from the 60S subunit) and translation initiation factors, including components of eIF4F translation initiation and cap-binding complex, eIF4G and two paralogs of eIF4A, eIF4AI and eIF4AII. Although eIF4F subunits were shown to associate with NMD factors in different organisms their role in this process is unclear (Rufener and Mühlemann et al. 2013). Together, our data are consistent with a notion that in plants, as in other organisms, NMD is coupled with translation initiation machinery.

Among proteins enriched in our analysis we also found proteins related to import into nucleus and vesicle-mediated transport, such as components of the nuclear pore as well as Golgi-associated COPI and COPII vesicle coat and clathrin-coated vesicle. The presence of UPF1 in a physical proximity to Golgi vesicles is in line with the interactome-mass spectrometry data of NMD factors in human cells (Schweingruber et al. 2016). Moreover, previously identified NMD factors NBAS and SEC13 (Anastasaki et al. 2011, Longman et al. 2013, Casadio et al. 2015) have been reported to associate with retrograde transport complexes from Golgi to ER (Tang et al. 1997, Aoki et al. 2009).

Finally, we noticed that UPF1 also associates with other factors involved in pathways related to RNA and protein metabolism, namely TUDOR-SN proteins and deubiquitinating enzymes (DUBs). The outcome of these interactions is currently unclear but they support a wider contribution of NMD to regulation of gene expression than solely via RNA surveillance.

DEA(D/H)-box RNA helicases contribute to plant NMD

RNA helicases belonging to the DEA(D/H)-box helicase family (Table 2) were highly represented among UPF1co-purifying proteins (Table 1; Supplementary Table S1). RH11, RH37 and RH52 helicases, homologs of human DDX3, were retrieved with a high score in all three biological replicas. RH6 and RH8 and RH12 proteins represent the second enriched group and are homologs of the human DDX6/p54 or yeast Dhh1 family. Finally, RH14 and RH46 (homologs of human DDX5 and DDX17, and yeast Dbp2) and RH56/UAP56B (homolog of DDX39) also co-purified with UPF1, but with a lower score or were also present in control samples. These findings are consistent with a recent plant UPF1 interactome study that also identified homologs of DDX3, DDX6 and DDX5/17, further supporting their potential involvement in plant NMD (Supplementary Table S1, Chicois et al. 2018). DEA(D/H)-box helicases were further tested for their contribution to plant NMD. For simplicity, RH11, RH37 and RH52 homologs are referred to as the DDX3 group, RH6, RH8 and RH12 homologs as the DDX6 group, and RH14 and RH46 as the DDX5 group.

For Peer Review

To investigate the role of identified RNA helicases in plant NMD we applied the VIGS-NMD assay (Virus-Induced Gene Silencing agroinfiltration transient NMD), which allows for a quick and efficient testing of many potential NMD factors by transient transfection of *N. benthamiana* leaves (Kerényi et al. 2008). Briefly, the expression of tested genes was inactivated by VIGS and then the NMD activity in silenced plants was assessed by measuring the level of transiently expressed GFP-based NMD sensitive reporter constructs. Simultaneous co-silencing of the endogenous phytoene desaturase (*PDS*) gene that leads to leaf bleaching phenotype allows estimation of silencing efficiency by the leaf bleaching phenotype (Fig. 1). VIGS silencing of *N. benthamiana DDX3*, *DDX5* and *DDX6* homologs and *PDS* in photobleached plants was checked by RT-qPCR (Supplementary Fig. S2). The levels of all six *DDX3* and four *DDX6 N. benthamiana* helicases were significantly reduced in VIGS plants. In contrast, although *PDS* level was similarly down regulated in these experiments, silencing of the DDX5 group was ineffective, probably due to a high number (12) of paralogs. VIGS experiments were carried out primarily for DDX3 and DDX6 helicases, but as silencing can occur also at a post-transcriptional level we also analysed NMD efficiency in DDX5-silenced plants. UPF1-PDS co-silenced (referred to as UPF1-silenced) line was used as an NMD-deficient positive control, while PDS silencing was used as negative control. To avoid general RNA silencing induced by agroinfiltration, each construct was co-transfected with the P14 suppressor that inhibits silencing but does not interfere with NMD. Expression of the NMD reporter construct encoding *GFP* mRNA with a 600 nt long 3'UTR region (G600) and the G95 non-NMD control was monitored at the protein level by GFP fluorescence in leaves and at the mRNA level by northern blotting, with P14 mRNA used as a normalization control. In control PDS-silenced plants, the G95 construct was expressed, while the level of the NMD-sensitive G600 mRNA was low due to NMD activity. In contrast, in UPF1-silenced plants where NMD is inhibited, high fluorescence was observed for both GFP reporters, with the G600 mRNAs levels 8 to 14 fold higher (depending on the experiment) than in control plants (Fig. 1A, B).

Since helicases in each group show a high amino acid sequence identity (from 71% up to 85%) (Supplementary Fig. S3; Supplementary Table S3), we expected they might act redundantly. Accordingly, the level of G600 NMD-sensitive reporter was not affected upon initial silencing of single members of the DDX3 family, RH11 or RH52 (Supplementary Fig. S4A). Therefore we decided to silence all homologs of each subfamily in *N. benthamiana* (Supplementary Tables S3, S4). Using the VIGS-NMD assay we observed that knock-down of DDX3 helicases led to a significant 8-fold accumulation of G600 NMD-sensitive reporter mRNA compared to the control (Fig. 1A, right panel; Supplementary Fig. S5A). This result suggests that helicases from the DDX3 are required for long 3'UTR-based NMD in plants. Surprisingly, the GFP fluorescence of G600-infiltrated DDX3-silenced leaves was similar to that of PDS-silenced negative control plants and

For Peer Review

not to the UPF1-silenced positive control (Fig. 1A, left panel). Lack of correlation between the level of G600 mRNA and the protein in DDX3-silenced leaves suggests that these helicases may also contribute to mRNA export or translation. Since NMD is a translation-coupled mechanism, the simplest explanation of this observation is that the DDX3 knock-down stabilizes NMD target mRNA while at the same time suppresses its translation, which results in reduced protein synthesis. Notably, human DDX3 is involved in multiple aspects of mRNA metabolism, including transcription, pre-mRNA splicing, mRNP assembly and translation (reviewed in Sharma and Jankowsky, 2014). The more general activity of plant DDX3 helicases is supported by a modest up-regulation (about 1.8-fold) of the G95 non-NMD control RNA upon DDX3 silencing (Fig. 1A, right panel). Similar effects have not been observed in the *rh11* mutant for four tested NMD targets, but inactivation of only one of the three DDX3 family helicases was assayed, indicating the possible redundancy of these proteins (Chicois et al. 2018).

In contrast to DDX3 helicases, silencing of DDX6 and DDX5 resulted in a decrease of the NMD-sensitive substrate (Fig.1B; Supplementary Fig. S4B, S5B, C). Since the effects of the DDX6 knock-down were stronger than those of the DDX5 knock-down and statistically significant, which is probably due to inefficient silencing of the DDX5 group (see Supplementary Fig. S2), we focused on the DDX6 helicase family. To confirm the observation that DDX6 helicases have an inhibitory effect on NMD, we transiently overexpressed RH12 helicase, which co-purified with UPF1 with the highest score. The level of the G600 reporter in RH12-overexpressing leaves was strongly up-regulated (4 fold) and it correlated well with a higher expression of the reporter GFP protein (Fig. 1C, right panel; Supplementary Fig. S5D). As a positive control, we overexpressed a UPF1 dominant-negative UPF1DN (U1DN) mutant variant, which inhibits NMD (Kertész et al. 2006), and this resulted in a strong up-regulation of G600 mRNA and enhanced GFP fluorescence (Fig.1C, Supplementary Fig. S5D).

To investigate unexpected NMD suppression by DDX6 helicases in the reporter VIGS assay we also analyzed accumulation of chosen endogenous NMD substrates in single *rh6-1, rh8-1*and *rh12-1*and double *rh8-1rh12-1, rh8-1 rh6-1* and *rh6-1 rh-12-1*Arabidopsis loss-of-function mutants (Supplementary Fig. S6), with the UPF1-deficient *upf1-5* line used as a positive control. A triple mutant lacking RH6, RH8 and RH12 is lethal. We tested the levels of *SMG7*, *AT5G45430*, *AT1G36730* mRNAs, which are NMD targets either due to a long 3'UTR that contains an intron (*SMG7*) or the presence of a uORF (*AT5G45430*, *AT1G36730*) (Rayson et al. 2012, Kerényi et al. 2008, Nyikó et al. 2013). RT-qPCR analysis showed a somewhat different outcome in 7-day-old and 14-day-old seedlings (Fig. 2A, B). In the first case, a marked down regulation of *AT5G45430* and *AT1G36730* mRNAs was observed in single mutants, with the most prominent effect in *rh12* plants, but no further enhancement was seen in double lines (Fig. 2A). In contrast, the level of all

For Peer Review

NMD substrates in 14-day-old seedlings was significantly decreased in double *ddx6* lines, but only slight changes were visible in single mutants (Fig. 2B). In general, these results are consistent with the decreased level of the reporter NMD substrate in DDX6-silenced *N. benthamiana* leaves (see Fig. 1B) and of two endogenous NMD targets in the *rh12* mutant (Chicois et al. 2018). These observations also suggest an interesting possibility that depending on the stage growth each of the DDX6 family paralogs may either have a more prominent contribution to NMD efficiency, as observed for RH12 helicase in 7-day-old seedlings, or they may act in a redundant fashion, as is the case in older seedlings. The strongest association of RH12 with UPF1 and its expression across all developmental stages and tissues in Arabidopsis (Klepikova et al. 2016, Supplementary Fig. S7) suggest that it may play a more important role in NMD.

To confirm the interaction of RH12 helicase with NMD core factors we carried out co-immunoprecipitation of GFP-tagged RH12 with HA-tagged UPF1 and UPF3 in *N. benthamiana* leaves infiltrated with a combination of constructs encoding these proteins. RH12-GFP was detected in the UPF1-HA immunoprecipitated fraction, supporting RH12 interaction with UPF1 (Supplementary Fig. S8). There was no RH12-HA signal in theUPF3-HA immunoprecipitate, perhaps indicating a more transient interaction or partial degradation of UPF3 during the co-IP procedure.

Together, these data show that at least two of DEA(D/H)-box RNA helicase families, homologs of DDX3 and DDX6 are directly involved in NMD regulation, and act with opposing impacts on NMD efficiency. It is possible that DDX5 group also contributes to NMD efficiency but to a lesser extent.

Co-localization of DEA(D/H)-box RNA helicases with UPF1 and UPF3

In plants, UPF1 was reported to localize in the cytoplasm, P-bodies and siRNA-bodies, whereas UPF3 is found in the nucleolus and cytoplasmic foci (Kim et al. 2009, Kerényi et al. 2013, Moreno et al. 2013, Chicois et al. 2018). We have also shown that UPF1 and SMG7 co-localize in P-bodies, suggesting that NMD targets may be targeted to these cytoplasmic dynamic structures at some stage in the process (Kerényi et al. 2013).

To further assess the role of RNA helicases in NMD we analyzed localization of selected helicases from the three DEA(D/H)-box subfamilies and their co-localization with core NMD factors, UPF1 and UPF3 (Figs. 3, 4; Supplementary Fig. S9). Localization of RH12-CFP (DDX6 group) and RH14-CFP (DDX5 group) was tested in transiently transfected Arabidopsis protoplasts, whereas RH11-CFP (DDX3 group) was tested in *N. benthamiana* leaves, as its expression in Arabidopsis protoplasts resulted in protein aggregation. We confirmed the presence of UPF1 in cytoplasmic foci and observed that UPF3 localized mostly to the nucleolus, but was also visible in

For Peer Review

the nucleoplasm and in cytoplasmic foci, most likely P-bodies (Fig. 3A; Supplementary Fig. S9). The RH12 helicase localized to the nucleus but was excluded from the nucleolus. We also detected it in the cytoplasm and in cytoplasmic foci that represent plant P-bodies, RH12 was previously reported to co-localize with DCP1, a component of these structures (Fig. 3B; Xu et al. 2006, Bhullar et al. 2017, Chicois et al. 2018). These results are consistent with the localization of DDX6 in human cells, where it plays a central role in P-body assembly in the cytoplasm and is also present in the nucleus (Ayache et al. 2015, Huang et al. 2017). As expected, RH12 co-localized with UPF1 and UPF3 in the cytoplasm and P-bodies and with UPF3 in the nucleoplasm (Fig. 3B). The DDX5 subfamily member RH14 was present primarily in the nucleolus and nucleoplasm and to some extent in cytoplasmic foci, where it overlapped with UPF1 (Fig. 3C). In the case of the DDX3 homolog RH11, we observed a strong fluorescent signal in the nucleus, nucleolus and cytoplasm (Fig. 4). In contrast to clear P-body distribution of RH12 (compare with RH12 localization in *N. benthamiana,* Supplementary Fig. S9), localization of RH11 in cytoplasmic foci was less evident. When RH11 was co-expressed with UPF1, the signal from both proteins fully overlapped in the cytoplasm and cytoplasmic foci. Similarly, when expressed together, RH11 and UPF3 co-localized mainly in the nucleolus but also in the nucleus.

These co-localization results strongly support co-immunoprecipitation and functional data that DDX3 and DDX6 subfamilies of DEA(D/H)-box helicases may act as regulatory factors in plant NMD. We speculate that they may associate with NMD factors (UPF3) already in the nucleoplasm and function in different stages of this process.

DISCUSSION

To examine the network of NMD factors in plants we identified proteins, which co-purify with *Arabidopsis* UPF1. Our results revealed known major NMD factors UPF2 and UPF3 as well as poly(A)-binding proteins PAB2, PAB3, PAB4 and PAB8 that were also identified in complex with UPF1 in humans and Arabidopsis (Schweingruber et al. 2016, Chicois et al. 2018). In addition, we found several translation initiation factors and ribosomal proteins, supporting the hypothesis that UPF1 might be recruited to mRNA via its interaction with the ribosome during translation initiation through association with ribosomal proteins (reviewed in Brogna et al. 2016).

UPF1 is a multifunctional protein, which, in addition to NMD mechanism, plays a role in other processes, either related or unrelated to NMD. Consistently, we found that UPF1 interacted with splicing and translation factors, as well as enzymes involved in RNA decay (Tudor-SN) and protein modification and degradation (deubiquitinating enzymes and, with a lower score, also proteasome subunits; see Supplementary Table S1). In human cells UPF1 has been reported to trigger Tudor-SN-mediated microRNA decay by stimulating their dissociation from mRNA targets

For Peer Review

(Elbarbar et al. 2017, reviewed in Kim and Maquat, 2019). Tudor-SN functions in many aspects of RNA metabolism and is a component of P-bodies and stress granules, also in Arabidopsis (Gutierrez-Beltran et al. 2015), supporting the notion that UPF1 may contribute to translation repression that occurs in these structures (Chicois et al. 2018). In turn, DUBs, among other functions, participate in proteasomal degradation by removing polyubiquitin chains from proteasome substrates. Notably, UPF1 in yeast was shown to activate rapid proteasomal degradation of truncated polypeptides that are produced by PTC-containing mRNAs (Kuroha et al. 2009) and one of the proteins that co-purify with UPF1 in *C. elegans* is a core subunit of the proteasome (Casadio et al. 2015). Interestingly, UBP12 and UBP13 DUBs as well as NMD factors, including UPF1, were implicated to act as negative regulators in Arabidopsis immune response (Ewan et al. 2011, Jeong et al. 2011, Rayson et al. 2012, Riehs-Kearnan et al. 2012, Gloggnitzer et al. 2014). These observations suggest that plant UPF1 may also have additional functions in RNA and protein homeostasis that impact physiological activities via pathways mediated by microRNAs and protein modification and stability.

Surprisingly, UPF1-interacting proteins did not reveal any kinase or kinases, which trigger NMD through UPF1 phosphorylation (this work, Chicois et al. 2018), especially considering that SMG1 co-purified with UPF1 in human cells (Kashima et al. 2006, Schweingruber et al. 2016). This indicates that either interaction between UPF1 and kinase(s) is transient or that the putative redundancy between several kinases acting on UPF1 makes their detection more difficult. Alternatively, despite its existence, UPF1 phosphorylation occurs at a low level and is not strictly required for NMD activation in *A. thaliana*, being replaced by other factors or mechanisms. Alternatively, UPF1 phosphorylation is dispensable for NMD activation in *A. thaliana* and, being replaced by other mechanisms (reviewed in Lloyd, 2018), is a residual feature and occurs at a very low level.

Among UPF1 interactors that represent potential auxiliary NMD factors and regulators we identified several DEA(D/H)-box RNA helicases. These proteins are part of a large family of ATPases that rearrange RNA secondary structures and thus remodel ribonucleoprotein complexes. DEA(D/H)-box helicases are involved in many aspects of RNA metabolism, such as ribosome biogenesis, spliceosome assembly, RNA decay and RNA editing (reviewed in Jarmoskaite and Russell, 2014). In our analyses we focused on UPF1-interacting helicases from three subfamilies, homologs of human DDX3, DDX5 and DDX6. These helicases were found in a complex with human UPF1, suggesting that their role in NMD is evolutionarily conserved (Geißler et al. 2013, Ayache et al. 2015, Flury et al. 2014, Schweingruber et al. 2016). Consistently, helicases from all three families (RH6, RH8 and RH12 from DDX6, RH11 from DDX3, and RH14 from DDX5) were also recovered among UPF1 co-purifying proteins from Arabidopsis flowers (Chicois et al. 2018).

For Peer Review

Human DDX5 has been reported to regulate the expression of selected mRNAs via NMD activation (Geißler et al. 2013), whereas the precise roles of DDX3 and DDX6 in NMD has not been demonstrated beyond their interaction with the NMD machinery. Analysis of a number of endogenous NMD targets in single helicase mutants from the three families in Arabidopsis did not provide clear evidence of their involvement in plant NMD (Chicois et al. 2018). We have shown that silencing of all homologs of DDX3 in *N. benthamiana* affects NMD efficiency, suggesting that helicases from this family may act redundantly as positive regulators of plant NMD. Interestingly, the change in the level of the NMD-sensitive reporter mRNA upon DDX3 silencing did not correlate with the expression of the corresponding protein, implying that the contribution of helicases from this family to NMD may involve regulation of translation. This possibility is supported by observations that human DDX3 helicase enhances translation initiation of mRNAs with structured 5'UTRs, possibly via interaction with the poly(A)-binding protein PABPC1 and several translation initiation factors (Soto-Rifo et al. 2012, reviewed in Soto-Rifo and Ohlmann, 2013). Our DDX6 silencing and overexpression experiments suggest that Arabidopsis DDX6 homologs function in NMD as negative regulators. This activity of DDX6 helicases is in line with the established role of metazoan DDX6 in translation repression, mRNA decay and P-body assembly (Hubstenberger et al. 2017, reviewed in Ostareck et al. 2014, Standart and Weil, 2018). Although RNA helicases have not been previously implicated in NMD suppression, we envisage that their RNA-protein remodeling activity may impede the assembly of the active NMD complex or promote more efficient translation termination with the assistance of poly(A)-binding proteins. Notably, PABP are well-documented termination-promoting factors and human PABPC1 has been shown to antagonize NMD by association with eIF4G (Fatscher et al. 2014, Joncourt et al. 2014, Ivanov et al. 2016). The regulatory capacity of DDX3 and DDX6 helicases in NMD through their interaction with PABPs and translation initiation factors are strongly supported by their co-purification in the UPF1 complex (this work, Chicois et al. 2018). Despite these findings, the mechanism of DDX3- and DDX6-mediated regulation of NMD is still unclear. We favor a model whereby DDX3 homologs stimulate the translation of NMD targets and in this way promote their degradation via a translation-coupled NMD mechanism. In turn, the action of DDX6 homologs is to suppress NMD, possibly by translation repression, to safeguard against excessive mRNA decay, in particular of NMD-insensitive transcripts. This represents a fine-tuning mechanism to balance NMD activity in degradation of aberrant PTC-containing substrates and regulation of expression of normal mRNAs.

The cellular distribution of DEA(D/H)-box helicases from the DDX3 and DDX6 families in the cytoplasm and P-bodies and their co-localization with the UPF complex is consistent with their role in both NMD (this work) and P-body assembly and function (Chicois et al. 2018). Moreover,

For Peer Review

co-localization of these helicases with UPF3 in the nucleus suggests that they are recruited at an early step of NMD, possibly during substrate recognition, which may be initiated already in the nucleus (Karousis and Mühlemann, 2018). Notably, nuclear localization of DDX3 and DDX6 helicases was also observed in human cells (Ayache et al. 2015, Huang et al. 2017, Brennan et al. 2018) and UPF1 was reported to associate with nascent transcripts in Drosophila in the nucleus where it starts scanning pre-mRNAs during their assembly into mRNP complexes (Singh et al. 2019). Localization of the RH14 helicase from the DDX5 subfamily mainly in the nucleus and nucleolus points to its possible involvement in regulation of transcription, pre-mRNA splicing, micro RNA biogenesis and/or rRNA processing, as is the case for human DDX5 (reviewed in Bourgeois et al. 2016). Its co-localization with UPF1 in cytoplasmic foci hints that DDX5 helicases may contribute to UPF1-related activities, possibly in NMD, as reported in human cells (Geißler et al. 2013); however, based on our analysis of DDX5-silenced plants, we cannot conclusively assert that this is indeed the case.

Distribution of NMD factors in the cytoplasm, nucleus, nucleolus and P-bodies brings the question about location of this process within the cell. The most likely scenario assumes that NMD is initiated in the nucleus by marking the substrates, while the majority of translation-dependent steps occur in the cytoplasm (Karousis and Mühlemann, 2018). In plants this scheme is preserved, with the possible involvement of a nucleolar phase (reviewed in Dai et al. 2016, Kim et al. 2009). Cytoplasmic mRNA degradation was at some point proposed to take place in P-bodies, where several mRNA decay factors, including the NMD complex, reside (reviewed in Chantarachot and Bailey-Serres, 2018, Standart and Weil, 2018). Recent data argue against this possibility and provide evidence that these dynamic structures accumulate translationally repressed rather than decayed mRNAs and are unlikely a major site for mRNA degradation (Schütz et al. 2017, Horvathova et al. 2017, Hubstenberger et al. 2017, reviewed in Tutucci et al. 2018). In this view, the presence of UPFs and UPF-interacting proteins (this work, Chicois et al. 2018) in P-bodies is puzzling; however, their association with repressed mRNAs may reflect the transient nature of mRNP storage that allows their release to polysomes for translation or degradation. Still, at the moment the notion that active NMD to some extent operates in P-bodies on a fraction of transcripts cannot be excluded.

In summary, UPF1 interaction network combined with functional and localization studies provide compelling evidence for the activity of DDX3 and DDX6 DEA(D/H)-box RNA helicases as NMD regulators, with opposing effects, either stimulatory or inhibitory, on NMD efficiency. Since NMD is important not only to eliminate aberrant transcripts but also to control the expression of natural transcripts (reviewed in Hug at al. 2016), NMD-associated RNA helicases acting as both positive and negative regulators of this process may contribute to optimal modulation of its capacity

For Peer Review

to meet cell requirements. NMD modulation could be particularly relevant in stress response, where stress signals repress NMD to enhance the expression of stress factors, and NMD hyperactivation may block efficient induction of the stress response (reviewed in He and Jacobson, 2015, Lykke-Andersen and Jensen, 2015, Hug at al. 2016). In addition, fine-tuning of NMD efficiency may be critical for specific mRNA classes, for example those with long 3'UTRs that need to evade degradation by NMD. Finally, regulated NMD events may provide a feedback to nuclear steps in gene expression and in this way have a more global impact on shaping the cellular transcriptome and proteome.

For Peer Review

Materials and methods

Plant material and growth condition

Wild-type (ecotype Col-0) and *upf1-5* (SALK_112911, a gift from Brendan Davies, University of Leeds), *rh6-1* (SAIL_111H08), *rh8-1* (GABI_447_H07), *rh12-1* (SALK_148563) and double *rh8-1rh12-1, rh8-1 rh6-1* and *rh6-1 rh-12-1*Arabidopsis plants were used in this study. Double mutants were created by crossing and plants were selected by PCR genotyping. A triple mutant with loss-of-function of RH6, RH8 or RH12 helicases is likely to be either male or female gametophytic lethal. *Arabidopsis thaliana* seeds were surface sterilized with 30% bleach 0.02% Triton-X100 solution and grown on Murashige and Skoog (MS) medium supplemented with 1% (w/v) sucrose and 0.3% phytagel, under a 16 h light/8 h dark (long-day) photoperiod. UPF1-SF-TAP (2xStrep-FLAG) transgenic lines expressing UPF1 protein under the control of the native promoter were generated by transforming *upf1-5* plants with *Agrobacterium tumefaciens* strain GV3101 carrying the pGWB604-UPF1-C-SF-TAP plasmid. Seeds from *A. tumefaciens*-treated plants were selected with 50 mg/mL of herbicides BASTA.

Affinity protein purification and mass spectrometry

UPF1-SF-TAP was purified as described (Golisz et al. 2013) with minor modifications. Detailed purification procedure and proteomic analysis are described in Supplementary Methods.

The VIGS-NMD assay and the agroinfiltration-based NMD tests system

Agroinfiltration and GFP detection were performed as described (Kertész et al. 2006 and Kerényi et al. 2013). Wild-type or silenced *N. benthamiana* leaves were infiltrated with a mixture of agrobacterial cultures (at OD_{600}=0.4 or at OD_{600}=0.2 in the case of P14). The GFP fluorescence was detected using a long-wave ultraviolet lamp. To trigger VIGS, 21-days-old *N. benthamiana* plants were co-infiltrated with a mixture of three *Agrobacterium* cultures expressing P14, TRV RNA1 and TRV RNA2 with segments of *N. benthamiana PDS*, *PDS+UPF1*, *PDS+DDX3*, *PDS+DDX5* or *PDS+DDX6* genes, respectively. PDS co-silencing is used to monitor silencing and expression of the P14 silencing suppressor serves to prevent activation of agroinfiltration-induced silencing, P14 mRNA is also used as an internal control for northern blots (Benkovics et al. 2011, Mérai et al. 2012). For the VIGS-NMD assay, *N. benthamiana* leaves 14 days post-silencing were agroinfiltrated with a mixture of cultures expressing P14 control and either G-600 NMD reporter or G-95 NMD insensitive construct. To assess the effect of protein overexpression, *N. benthamiana* leaves were agroinfiltrated with a mixture of cultures expressing P14 internal control, the overexpression construct (UPF1DN or R12 helicase) and either G600 NMD reporter or G-95 NMD insensitive control. VIGS efficiency assay was performed as previously described (Kerényi et al. 2008, Mérai, et al. 2013 and Nyikó et al. 2017).

RNA methods

For Peer Review

Total RNA was isolated from 2-week-old seedlings using Trizol reagent (Sigma) according to the manufacturer's instructions. Northern blotting was performed exactly as described (Kertész et al. 2006, Golisz et al. 2013) with random primed probes amplified on PCR fragments corresponding to *GFP* (the coding region of G-95 and G-600) or *P14* sequences and labeled using DECAprime™ II labeling kit (Ambion). Quantification was performed using a Storm 860 PhosphorImager (GE Healthcare) and ImageQuant software (Molecular Dynamics). For RT-qPCR cDNA was prepared with a mix of oligo(dT)$_{20}$ (Invitrogen) and 10xRT Random Primers (Invitrogen) using a SuperScript® IV Reverse Transcriptase Kit (Sigma) for 10 min at 65ºC on 25 µg of total RNA treated with RNase-free TURBO DNase (Ambion) for 60 min at 37ºC. qPCR was carried out using LightCycler® 480 SYBR Green I Master (Roche). The ubiqutin (AT4G2760) mRNA was used for normalization of relative expression values. All reactions were run at least in three independent biological replicates with the same result.

Co-immunoprecipitation assay

Co-IP was carried out as described (Kerényi et al. 2008) using *N. benthamiana* leaves co-infiltrated with constructs expressing RH12-GFP and UPF1-HA or UPF3-HA. Anti-HA affinity matrix (Roche) was used for IPs. Mouse monoclonal antibodies anti-HA peroxidase (Roche) and anti-GFP peroxidase (Santa Cruz) were used for chemiluminescence protein detections according to the manufacturer's instructions (ECL, Amersham - Biosciences).

Western blotting

Proteins from plant extracts were separated by SDS-PAGE gels and electrotransferred on polyvinylidene fluoride membranes (Immobilon, Millipore). Western hybridizations were performed with rabbit polyclonal antibodies against RH6 (1:2000), RH8 (1:500), RH12 (1:3000) produced by Eurogentec (Belgium) using double X immunization program. Anti-rabbit (Sigma) horseradish peroxidase-conjugated antisera were used as secondary antibodies.

Subcellular localization

UPF1, UPF3, RH11, RH12 and RH14 proteins were fused to protoplasts localization-optimized variants of cyan and yellow fluorescent protein (CFP and YFP) (Kremers et al. 2006, Kerényi et al. 2013). Arabidopsis mesophyll protoplasts were prepared from 14-days-old seedlings and transfected with plasmid DNA as described (Wu et al. 2009, Nyikó et al. 2013). For localization in *N. benthamiana* 5-week-old leaves were infiltrated with Agrobacterium carrying UPF1-YFP, UPF3-YFP, RH11-CFP and RH12-CFP binary plasmids. Arabidopsis protoplasts following 20-24 h incubation or *N. benthamiana* leaves 3 days after infiltration were imaged using a FluoView1000 confocal system (Olympus, http://www.olympus.com/) on an inverted IX81 microscope, using a PLANAPO 60.0 9 /1.2 water objective. The CFP emission, YFP emission and chlorophyll

For Peer Review

autofluorescence were detected at emission spectra of 460-500 nm, 530-590 nm and 655-755, respectively, after excitation at 440 nm for CFP and 515 nm for YFP and chlorophyll.

Funding

This work was supported by National Science Centre [UMO-2012/05/D/NZ1/00030 and UMO-2014/15/B/NZ2/02302] to JK; National Science Centre [UMO-2018/28/T/NZ1/00077 and UMO-2015/19/N/NZ2/00200] and EMBO Short-Term Fellowship [ASTF-396-2015 and STF-7351] to AS; Agence Nationale de la Recherche [ANR-14-CE10-0015, ANR-3'ModRN: ANR-15-CE12-0008-12] to CB-A, and National Research, Development and Innovation Office [NKFIH-K 129177] to DS. Experiments were carried out with the use of CePT infrastructure financed by the European Union-the European Regional Development Fund Innovative economy 2007-13, [AGREEMENT POIG.02.02.00-14-024/08-00S].

Disclosures

No conflicts of interest declared.

Acknowledgments

We thank John W. S. Brown (University of Dundee, UK) for pENTR1A plasmid and Jan W. Borst for pGD vector (Wageningen University, Netherlands).

References

Anastasaki, C., Longman, D., Capper, A., Patton, E.E. and Cáceres, J.F. (2011) Dhx34 and Nbas function in the NMD pathway and are required for embryonic development in zebrafish. *Nucleic Acids Res.* 39: 3686–3694.

Aoki, T., Ichimura, S., Itoh, A., Kuramoto, M., Shinkawa, T. and Isobe, T. (2009) Identification of the neuroblastoma-amplified gene product as a component of the syntaxin 18 complex implicated in Golgi-to-endoplasmic reticulum retrograde transport. *Mol. Biol. Cell*, 20: 2639–2649.

Arciga-Reyes, L., Wootton, L., Kieffer, M. and Davies, B. (2006) UPF1 is required for nonsense-mediated mRNA decay (NMD) and RNAi in Arabidopsis. *Plant J.* 47: 480–489.

Ayache, J., Bénard, M., Ernoult-Lange, M., Minshall, N., Standart, N., Kress, M. et al. (2015) P-body assembly requires DDX6 repression complexes rather than decay or Ataxin2/2L complexes. *Mol. Biol. Cell*, 26: 2579–2595.

For Peer Review

Benkovics, A.H., Nyikó, T., Mérai Z., Silhavy, D. and Bisztray, G.D. (2011) Functional analysis of the grapevine paralogs of the SMG7 NMD factor using a heterolog VIGS-based gene depletion-complementation system. *Plant Mol. Biol*. 75: 277–290.

Bhullar, D.S., Sheahan, M.B. and Rose, R.J. (2017) RNA processing body (P-body) dynamics in mesophyll protoplasts re-initiating cell division. *Protoplasma*, 254: 1627–1637.

Bourgeois, C.F., Mortreux, F. and Auboeuf, D. (2016) The multiple functions of RNA helicases as drivers and regulators of gene expression. *Nat. Rev. Mol. Cell. Bio.* 17: 426–438.

Brennan, R., Haap-Hoff, A., Gu, L., Gautier, V., Long, A. and Schröder M. (2018) Investigating nucleo-cytoplasmic shuttling of the human DEAD-box helicase DDX3. *Eur. J. Cell. Biol.* 97: 501–511.

Brogna, S., McLeod, T. and Petric, M. (2016) The Meaning of NMD: Translate or Perish. *Trends Genet.* 32: 395–407.

Casadio, A., Longman, D., Hug, N., Delavaine, L., Vallejos-Baier, R. and Alonso, C.R. (2015) Identification and characterization of novel factors that act in the nonsense-mediated mRNA decay pathway in nematodes, flies and mammals. *EMBO Rep*. 16: 71–78.

Causier, B., Li, Z., De Smet, R., Lloyd, J.P.B., Van de Peer, Y. and Davies B. (2017) Conservation of Nonsense-Mediated mRNA Decay complex components throughout eukaryotic evolution. *Sci Rep-UK.* 7: 16692.

Celik, A., He, F. and Jacobson, A. (2017) NMD monitors translational fidelity 24/7. *Curr. Genet.* 63: 1007–1010.

Chantarachot, T. and Bailey-Serres, J. (2018) Polysomes, Stress Granules, and Processing Bodies: A dynamic triumvirate controlling cytoplasmic mRNA fate and function. *Plant Physiol*. 176: 254–269.

Chicois, C., Scheer, H, Garcia, S., Zuber, H., Mutterer, J., Chicher, J., et al. (2018) The UPF1 interactome reveals interaction networks between RNA degradation and translation repression factors in Arabidopsis. *Plant J.* 96: 119–132.

Cho, H., Han, S., Choe, J., Park, S.G., Choi, S.S. and Kim, Y.K. (2013) SMG5-PNRC2 is functionally dominant compared with SMG5-SMG7 in mammalian nonsense-mediated mRNA decay. *Nucleic Acids Res.* 41: 1319–1328.

Cui, P., Chen, T., Qin, T., Ding, F., Wang, Z., Chen, H., et al. (2016) The RNA polymerase II C-terminal domain phosphatase-like protein FIERY2/CPL1 interacts with eIF4AIII and is essential for nonsense-mediated mRNA decay in Arabidopsis. *Plant Cell*, 28: 770–785.

Dai, Y., Li, W. and An, L. (2016) NMD mechanism and the functions of Upf proteins in plant. *Plant Cell Rep.* 35: 5–15.

For Peer Review

Drechsel, G., Kahles, A., Kesarwani, A.K., Stauffer, E., Behr, J., Drewe, P., et al. (2013) Nonsense-mediated decay of alternative precursor mRNA splicing variants is a major determinant of the Arabidopsis steady state transcriptome. *Plant J.* 25: 3726–3742.

Elbarbary, R.A., Miyoshi, K., Hedaya, O., Myers, J.R. and Maquat, L.E. (2017) UPF1 helicase promotes TSN-mediated miRNA decay. *Gene Dev.* 31:1–11.

Ewan, R., Pangestuti, R., Thornber, S., Craig, A., Carr, C., O'Donnell, L., et al. (2011) Deubiquitinating enzymes AtUBP12 and AtUBP13 and their tobacco homologue NtUBP12 are negative regulators of plant immunity. *New Phytol.*191: 92–106.

Fanourgakis, G., Lesche, M., Akpinar, M., Dahl, A. and Jessberger, R. (2016) Chromatoid body protein TDRD6 supports long 3' UTR triggered Nonsense Mediated mRNA Decay. *PLoS Genet.* 12: e1005857.

Fatscher, T., Boehm, V., Weiche, B. and Gehring, N.H. (2014) The interaction of cytoplasmic poly(A)-binding protein with eukaryotic initiation factor 4G suppresses nonsense-mediated mRNA decay. *RNA,* 20: 1579–1592.

Flury, V., Restuccia, U., Bachi, A. and Mühlemann, O. (2014) Characterization of phosphorylation- and RNA-dependent UPF1 interactors by quantitative proteomics. *J. Proteome Res.* 13: 3038–3053.

Geißler, V., Altmeyer, S., Stein, B., Uhlmann-Schiffler, H. and Stahl, H. (2013) The RNA helicase Ddx5/p68 binds to hUpf3 and enhances NMD of Ddx17/p72 and Smg5 mRNA. *Nucleic Acids Res.* 41: 7875–7888.

Gloggnitzer, J., Akimcheva, S., Srinivasan, A., Kusenda, B., Riehs, N., Stampfl, H., et al. (2014) Nonsense-mediated mRNA decay modulates immune receptor levels to regulate plant antibacterial defense. *Cell Host Microbe,* 16: 376–390.

Golisz, A., Sikorski, P.J., Kruszka, K. and Kufel, J. (2013) Arabidopsis thaliana LSM proteins function in mRNA splicing and degradation. *Nucleic Acids Res.* 41: 6232–6249.

Gregersen, L.H., Schueler, M., Munschauer, M., Mastrobuoni, G., Chen, W., Kempa, S., et al. (2014) MOV10 is a 5′ to 3′ RNA helicase contributing to UPF1 mRNA target degradation by translocation along 3′ UTRs. *Mol. Cell*, 54: 573–585.

Gutierrez-Beltran, E., Moschou, P.N., Smertenko, A.P. and Bozhkov PV. (2015) Tudor staphylococcal nuclease links formation of stress granules and processing bodies with mRNA catabolism in Arabidopsis. *Plant Cell,* 27: 926–43.

He, F. and Jacobson, A. (2015) Nonsense-Mediated mRNA Decay: degradation of defective transcripts is only part of the story. *Annu. Rev. Genet.* 49: 339–366.

Hori, K. and Watanabe, Y. (2005) UPF3 suppresses aberrant spliced mRNA in Arabidopsis. *Plant J.* 43: 530–540.

Horvathova, I., Voigt, F., Kotrys, A.V., Zhan, Y., Artus-Revel, C.G., Eglinger, J., et al. (2017) The dynamics of mRNA turnover revealed by single-molecule imaging in single cells. *Mol. Cell*, 68: 615–625.

Hu, W., Petzold, C., Coller, J. and Baker K.E. (2010) Nonsense-mediated mRNA decapping occurs on polyribosomes in *Saccharomyces cerevisiae*. *Nat. Struct. Mol. Biol.* 17: 244–724.

Huang, J.H., Ku, W.C., Chen, Y.C., Chang, Y.L. and Chu, C.Y. (2017) Dual mechanisms regulate the nucleocytoplasmic localization of human DDX6. *Sci. Rep-UK.* 7: 42853.

Hubstenberger, A., Courel, M., Bénard, M., Souquere, S., Ernoult-Lange, M., Chouaib, R., et al. (2017) P-Body purification reveals the condensation of repressed mRNA regulons. *Mol. Cell*, 68: 144–157.

Hug, N., Longman, D. and Cáceres, J.F. (2016) Mechanism and regulation of the nonsense-mediated decay pathway. *Nucleic Acids Res.* 44: 1483–1495.

Hug, N. and Cáceres, J.F. (2014) The RNA helicase DHX34 activates NMD by promoting a transition from the surveillance to the decay-inducing complex. *Cell Rep.* 8: 1845–1856.

Ivanov, A., Mikhailova, T., Eliseev, B., Yeramala, L., Sokolova, E., Susorov, D., et al. (2016) PABP enhances release factor recruitment and stop codon recognition during translation termination. *Nucleic Acids Res.* 44: 7766–7776.

Izumi, N., Yamashita, A., Iwamatsu, A., Kurata, R., Nakamura, H., Saari, B., et al. (2010) AAA+ proteins RUVBL1 and RUVBL2 coordinate PIKK activity and function in nonsense-mediated mRNA decay. *Sci. Signal.* 3: ra27.

Jarmoskaite, I. and Russell, R. (2014) RNA helicase proteins as chaperones and remodelers. *Annu. Rev. Biochem*. 83: 697–725.

Jeong, H.J., Kim, Y.J., Kim, S.H., Kim, Y.H., Lee, I.J., Kim, Y.K., et al. (2011) Nonsense-mediated mRNA decay factors, UPF1 and UPF3, contribute to plant defense. *Plant Cell Physiol.* 52: 2147–56.

Joncourt, R., Eberle, A.B., Rufener, S.C. and Mühlemann, O. (2014) Eukaryotic initiation factor 4G suppresses nonsense-mediated mRNA decay by two genetically separable mechanisms. *PLoS ONE*, 9: e104391.

Karousis, E.D. and Mühlemann, O. (2018) Nonsense-Mediated mRNA Decay begins where translation ends. *CSH Perspect. Biol*. pii: a032862.

Kashima, I., Yamashita, A., Izumi, N., Kataoka, N., Morishita, R., Hoshino, S., et al. (2006) Binding of a novel SMG-1-Upf1-eRF1-eRF3 complex (SURF) to the exon junction complex triggers Upf1 phosphorylation and nonsense-mediated mRNA decay. *Genes Dev*. 20: 355–67.

Kerényi, F., Wawer, I., Kufel, J., Sikorski, P.J. and Silhavy, D. (2013) Phosphorylation of the N- and C-terminal UPF1 domains plays a critical role in plant nonsense-mediated mRNA decay (NMD). *Plant J.* 76: 836–848.

Kerényi, Z., Mérai, Z., Hiripi, L., Benkovics, A., Gyula, P., Lacomme, C., et al. (2008) Interkingdom conservation of mechanism of nonsense-mediated mRNA decay. *EMBO J.* 27: 1585–1595.

Kertész, S., Kerényi, Z., Mérai, Z., Bartos, I., Pálfy, T., Barta E., et al. (2006) Both introns and long 3'-UTRs operate as cis-acting elements to trigger nonsense-mediated decay in plants. *Nucleic Acids Res.* 34: 6147–6157.

Kim, S.H., Koroleva, O.A., Lewandowska, D., Pendle, A.F., Clark, G.P., Simpson, C.G., et al. (2009) Aberrant mRNA transcripts and the nonsense-mediated decay proteins UPF2 and UPF3 are enriched in the Arabidopsis nucleolus. *Plant Cell*, 21: 2045–2057.

Kim, Y.K. and Maquat, L.E (2019) UPFront and center in RNA decay: UPF1 in nonsense-mediated mRNA decay and beyond. *RNA,* 25: 407–422.

Klepikova, A.V., Kasianov, A.S., Gerasimov, E.S., Logacheva, M.D. and Penin, A.A. (2016) A high resolution map of the Arabidopsis thaliana developmental transcriptome based on RNA-seq profiling. *Plant J.* 88: 1058–1070.

Kuroha, K., Tatematsu, T. and Inada, T. (2009) Upf1 stimulates degradation of the product derived from aberrant messenger RNA containing a specific nonsense mutation by the proteasome. *EMBO Rep.* 10: 1265–1271.

Lloyd, J.P.B, Lang D., Zimmer, A.D, Causier, B., Reski, R. and Brendan, D. (2018) The loss of SMG1 causes defects in quality control pathways in *Physcomitrella patens*. *Nucleic Acids Res.* 46: 5822–5836.

Lloyd, J.P.B. (2018) The evolution and diversity of the nonsense-mediated mRNA decay pathway. *Version 2. F1000 Res*. 7: 1299.

Lloyd, J.P.B. and Davies, B. (2013) SMG1 is an ancient nonsense-mediated mRNA decay effector. *Plant J*. 76: 800–810.

Loh, B., Jonas, S. and Izaurralde, E. (2013) The SMG5-SMG7 heterodimer directly recruits the CCR4-NOT deadenylase complex to mRNAs containing nonsense codons via interaction with POP2. *Genes Dev.* 27: 2125–2138.

Longman, D., Hug, N., Keith, M., Anastasaki, C., Patton, E.E., Grimes, G., et al. (2013) DHX34 and NBAS form part of an autoregulatory NMD circuit that regulates endogenous RNA targets in human cells, zebrafish and *Caenorhabditis elegans*. *Nucleic Acids Res.* 41: 8319–8331.

Longman, D., Plasterk, R.H., Johnstone, I.L. and Cáceres, J.F. (2007) Mechanistic insights and identification of two novel factors in the *C. elegans* NMD pathway. *Genes Dev*. 21: 1075–1085.

Lykke-Andersen, S. and Jensen, T.H. (2015) Nonsense-mediated mRNA decay: an intricate machinery that shapes transcriptomes. *Nat. Rev. Mol. Cell Biol.* 16: 665–677.

Melero, R., Hug, N., López-Perrote, A., Yamashita, A., Cáceres, J.F. and Llorca, O. (2016) The RNA helicase DHX34 functions as a scaffold for SMG1-mediated UPF1 phosphorylation. *Nat. Commun*. 7: 10585.

Mérai, Z., Benkovics, A.H., Nyikó, T., Debreczeny, M., Hiripi, L., Kerényi, Z., et al. (2013) The late steps of plant nonsense-mediated mRNA decay. *Plant J.* 73: 50-62.

Moreno, A.B., Martinez de Alba, A.E., Bardou, F., Crespi, M.D., Vaucheret, H. and Maizel, A. (2013) Cytoplasmic and nuclear quality control and turnover of single-stranded RNA modulate post-transcriptional gene silencing in plants. *Nucleic Acids Res*. 41: 4699–4708.

Morris, C., Wittmann, J., Jack, H.M. and Jalinot, P. (2007) Human INT6/eIF3e is required for nonsense-mediated mRNA decay. *EMBO Rep*. 8: 596–602.

Mühlemann, O. (2008) Recognition of nonsense mRNA: towards a unified model. *Biochem. Soc. T*. 36: 497–501.

Nagy, E. and Maquat, L.E. (1998) A rule for termination-codon position within intron-containing genes: when nonsense affects RNA abundance. *Trends Biochem. Sci*. 23: 198–199.

Nicholson, P. and Mühlemann, O. (2010) Cutting the nonsense: the degradation of PTC-containing mRNAs. *Biochem. Soc. T.* 38: 1615–1620.

Nyikó, T., Kerényi, F., Szabadkai, L., Benkovics, A.H., Major, P., Sonkoly, B., et al. (2013) Plant nonsense-mediated mRNA decay is controlled by different autoregulatory circuits and can be induced by an EJC-like complex. *Nucleic Acids Res.* 41: 6715–6728.

Ostareck, D.H., Naarmann-de Vries, I.S. and Ostareck-Lederer A. (2014) DDX6 and its orthologs as modulators of cellular and viral RNA expression. *WIRES RNA*, 5: 659–678.

Peccarelli, M. and Kebaara, B.W. (2014) Regulation of natural mRNAs by the nonsense-mediated mRNA decay pathway. *Eukaryot. Cell*, 13: 1126–1135.

Raxwal, V. K. and Riha, K. (2016) Nonsense mediated RNA decay and evolutionary capacitance. *Biochim. Biophys. Acta, Gene Regul. Mech*, 1859: 1538–1543.

Rayson, S., Arciga-Reyes, L., Wootton, L., De Torres Zabala, M., Truman, W., Graham, N., et al. (2012) A role for nonsense-mediated mRNA decay in plants: pathogen responses are induced in Arabidopsis thaliana NMD mutants. PLoS ONE, 7: e31917.

Riehs, N., Akimcheva, S., Puizina, J., Bulankova, P., Idol, R. A., Siroky, J., et al. (2006) Arabidopsis SMG7 protein is required for exit from meiosis. *J. Cell Sci*. 6: 2208–2216.

Riehs-Kearnan, N., Gloggnitzer, J., Dekrout, B., Jonak, C. and Riha, K. (2012). Aberrant growth and lethality of Arabidopsis deficient in nonsense-mediated RNA decay factors is caused by autoimmune-like response. *Nucleic Acids Res.* 40: 5615–5624.

Rufener, S.C. and Mühlemann, O. (2013) eIF4E-bound mRNPs are substrates for nonsense-mediated mRNA decay in mammalian cells. *Nat. Struct. Mol. Biol*. 20: 710–717.

Schoenberg, D.R. and Maquat, L.E. (2012) Regulation of cytoplasmic mRNA decay. *Nat. Rev. Genet*. 13: 246–259.

Schütz, S., Nöldeke, E.R. and Sprangers, R. (2017) A synergistic network of interactions promotes the formation of in vitro processing bodies and protects mRNA against decapping. *Nucleic Acids* Res. 45: 6911–6922.

Schweingruber, C., Rufener, S.C., Zund, D., Yamashita, A. and Mühlemann, O. (2013) Nonsense-mediated mRNA decay - mechanisms of substrate mRNA recognition and degradation in mammalian cells. *Biochim. Biophys. Acta, Gene Regul. Mech*, 1829: 612–623.

Schweingruber, C., Soffientini, P., Ruepp, M.D., Bachi, A. and Mühlemann, O. (2016) Identification of interactions in the NMD complex using proximity-dependent biotinylation (BioID). *PLoS ONE*, 11: e0150239.

Sharma, D. and Jankowsky, E. (2014) The Ded1/DDX3 subfamily of DEAD-box RNA helicases. *Crit. Rev. Biochem. Mol.* 49: 343–360.

Shaul, O. (2015) Unique aspects of plant Nonsense-Mediated mRNA Decay. *Trends Plant Sci.* 20: 767–779.

Singh, A.K., Choudhury, S.R., De, S., Zhang, J., Kissane, S., Dwivedi, V., et al. (2019) The RNA helicase UPF1 associates with mRNAs co-transcriptionally and is required for the release of mRNAs from gene loci. *Elife*. 8. pii: e41444.

Soto-Rifo, R. and Ohlmann T. (2013) The role of the DEAD-box RNA helicase DDX3 in mRNA metabolism. *WIRES RNA*. 4: 369–85.

Soto-Rifo, R., Rubilar, P. S., Limousin, T., de Breyne, S., Decimo, D. and Ohlmann, T. (2012) DEAD-box protein DDX3 associates with eIF4F to promote translation of selected mRNAs. *EMBO J*. 31: 3745–3756.

Souret, F.F., Kastenmayer, J.P. and Green, P.J. (2004) AtXRN4 degrades mRNA in Arabidopsis and its substrates include selected miRNA targets. *Mol. Cell*, 15: 173–183.

Standart, N. and Weil, D. (2018) P-Bodies: cytosolic droplets for coordinated mRNA storage. *Trends Genet.* 34: 612–626.

Tang, B.L., Peter, F., Krijnse-Locker, J., Low, S.H., Griffiths, G. and Hong, W. (1997) The mammalian homolog of yeast Sec13p is enriched in the intermediate compartment and is essential for protein transport from the endoplasmic reticulum to the Golgi apparatus. *Mol. Cell Biol*. 17: 256–266.

Tian, M., Yang, W., Zhang, J., Dang, H., Lu, X., Fu, Ch., et al. (2017) Nonsense-mediated mRNA decay in *Tetrahymena* is EJC independent and requires a protozoa-specific nuclease. *Nucleic Acids Res.* 45: 6848–6863.

Tutucci, E., Livingston, N.M., Singer, R.H. and Wu, B. (2018) Imaging mRNA *in vivo*, from birth to death. *Annu. Rev. Biophys.* 47: 85–106.

Wu, F.H., Shen, S.C., Lee, L.Y., Lee, S.H., Chan, M.T. and Lin, C.S. (2009) Tape-Arabidopsis Sandwich - a simpler Arabidopsis protoplast isolation method. *Plant Methods*, 5: 16.

Wu, J., Kang, J.H., Hettenhausen, C. and Baldwin, I.T. (2007) Nonsense-mediated mRNA decay (NMD) silences the accumulation of aberrant trypsin proteinase inhibitor mRNA in *Nicotiana attenuata*. *Plant J.* 51: 693–706.

Xu, J., Yang, J.Y., Niu, Q.W. and Chua, N.H. (2006) DCP2, DCP1, and VARICOSE form a decapping complex required for postembryonic development. *Plant Cell*, 18: 3386–3398.

For Peer Review

Table 1

	Acc. number	Name
1	AT5G47010	**UPF1**
2	AT1G54270	Eukaryotic translation initiation factor eIF4A-2
3	AT3G13920	Eukaryotic translation initiation factor eIF4A-1
4	AT1G26630	Eukaryotic translation initiation factor eIF5A-1
5	AT2G23350	Poly(A) binding protein PAB4
6	AT3G11130	Clathrin, heavy chain CHC1 (vesicle-mediated trafficking)
7	AT4G34110	Poly(A) binding protein 2 PAB2
8	AT2G39260	**UPF2**
9	AT4G10320	tRNA synthetase class I (I, L, M and V) family protein
10	AT1G49760	Poly(A) binding protein 8 PAB8
11	AT1G56070	Ribosomal protein S5/Elongation factor G/III/V family protein LOS1
12	AT2G41840	Ribosomal protein S5 family protein
13	AT5G05010	Clathrin adaptor complexes medium subunit family protein (vesicle-mediated transport)
14	AT3G49430	SER/ARG-rich protein SR34A
15	AT3G08530	Clathrin, heavy chain (vesicle-mediated trafficking)
16	AT1G02840	Serine/arginine-rich protein splicing factors SR34
17	AT3G63460	Transducin family protein/WD-40 repeat family protein (vesicle-mediated transport)
18	AT1G58983	Ribosomal protein S5 family protein
19	AT1G59359	Ribosomal protein S5 family protein
20	AT1G58380	Ribosomal protein S5 family protein
21	AT1G58684	Ribosomal protein S5 family protein
22	AT1G11650	RNA-binding (RRM/RBD/RNP motifs) family protein
23	AT5G61780	TUDOR-SN protein 2
24	AT5G02870	Ribosomal protein L4/L1 family RPL4
25	AT1G33980	**UPF3**
26	AT4G27000	RNA-binding (RRM/RBD/RNP motifs) family protein RBP45C
27	AT5G06600	Ubiquitin-specific protease 12
28	AT4G31480	Coatomer, beta subunit (vesicle-mediated transport)
29	AT4G31490	Coatomer, beta subunit (vesicle-mediated transport)
30	AT5G11170	DEAD/DEAH box RNA helicase family protein UAP 56a
31	AT5G11200	DEAD/DEAH box RNA helicase family protein UAP 56b
32	AT2G21390	Coatomer alpha subunit (vesicle-mediated transport)
33	AT3G11910	Ubiquitin-specific protease 13
34	AT1G27970	Nuclear transport factor 2B NTF2B
35	AT2G42520	P-loop containing nucleoside triphosphate hydrolases superfamily protein RH37
36	AT3G58570	P-loop containing nucleoside triphosphate hydrolases superfamily protein RH52
37	AT3G58510	DEA(D/H)-box RNA helicase family protein RH11
38	AT2G37270	Ribosomal protein 5B
39	AT3G11940	Ribosomal protein 5A
40	ATCG00770	Ribosomal protein S8
41	AT2G45810	DEA(D/H)-box RNA helicase family protein RH6
42	AT3G61240	DEA(D/H)-box RNA helicase family protein RH12
43	AT1G26910	Ribosomal protein L16p/L10e family protein RPL10B

For Peer Review

44	AT1G66580	Ribosomal protein L16p/L10e family protein RPL10C
45	AT3G11510	Ribosomal protein S11 family protein
46	AT1G05190	Ribosomal protein L6 family
47	AT3G25920	Ribosomal protein L15
48	AT5G39850	Ribosomal protein S4
49	AT1G22760	Poly(A) binding protein 3 PAB3
50	AT1G79850	Ribosomal protein S17
51	ATCG00820	Ribosomal protein S19
52	ATCG00750	Ribosomal protein S11
53	AT5G52040	Serine/arginine-rich protein splicing factors 41 RS41
54	AT5G07350	TUDOR-SN protein 1
55	AT3G60240	Eukaryotic translation initiation factor 4G eIF4G
56	AT4G00660	RNA helicase-like 8 RH8
57	AT3G01540	DEAD box RNA helicase RH14
58	AT5G14610	DEAD box RNA helicase RH46
59	AT4G25500	Arginine/serine-rich splicing factor 35
60	AT1G04170	Eukaryotic translation initiation factor 2 gamma subunit eIF2
61	AT5G20920	Eukaryotic translation initiation factor 2 beta subunit eIF2

Table 2

Acc. Number	Number of queries	Name	Human homologs	Yeast homologs
AT3G58510	2,2,2	RH11	DDX3	DED1, DBP1
AT2G42520	2,2,2	RH37		
AT3G58570	2,2,2	RH52		
AT3G61240	2,2	RH12	DDX6	DHH1
AT4G00660	3,1	RH8		
AT2G45810	3,2	RH6		
AT5G14610	2,1	RH46	DDX5	DBP2
AT3G01540	2,1	RH14 (DRH1)		

For Peer Review

Table legends

Table 1

Selected proteins that co-purify with UPF1

A list of the most interesting proteins related to RNA metabolism and/or NMD that were identified in at least two out of three replicas of UPF1-SF immunoprecipitations or enriched compared to negative control (Col-0 IP). Proteins highlighted in light blue represent proteins identified exclusively in UPF1 co-IP (not found in Col-0), DEA(D/H)-box RNA helicases chosen for further analysis are highlighted in pink. Proteins with the median difference between UPF1 co-IP and control samples > 0.0002 are separated by a black line from those with a median difference < 0.0002 or with a less than 2 identified peptides. Enrichment was estimated as a difference of medians calculated from normalized number of queries (see Supplementary Table S1).

Table 2

DEA(D/H)-box RNA helicases co-purifying with UPF1

Figure legends

Fig.1 Contribution of DDX3 and DDX6 helicases to plant NMD.

(A-B) VIGS-NMD assay in (A) DDX3-, or (B) DDX6- silenced *N. benthamiana* leaves that were co-infiltrated with P14 silencing suppressor and G95 NMD-insensitive or G600 NMD-sensitive substrates. PDS-silencing (PDS) and UPF1-PDS co-silencing (UPF) were used as a negative and positive control, respectively. (C) The level of reporter G95 and G600 substrates in RH12-overexpressing *N. benthamiana* leaves that were co-infiltrated with RH12 or U1DN constructs. Overexpression of UPF1 dominant negative form (U1DN) leads to inactivation of NMD and is used as a positive control. GFP fluorescence (top left panels) reflects the protein level and northern blots (bottom left panels) show the mRNA level. UV photos were taken and RNA isolated after 3 d.p.i. Northern blot was performed using *GFP* and *P14* probes. Graphical representation (right panels) of G95 or G600 transcript level from northern blots, P14 served as a normalization control. The level of G95 or G600 in silenced (A-B) or overexpressing (C) leaves are expressed relative to G95 or G600 in control leaves. Values represent a mean of three independent biological replicates with standard deviations shown by error bars (SD), *P < 0.05, **P < 0.01, ***P < 0.001 (t-test).

Fig. 2 Accumulation of endogenous NMD substrates in DDX6 mutants.

mRNA level of *SMG7*, *AT5G45430* and *AT1G36730* NMD endogenous substrates in Col-0*, upf1-5, rh6, rh8, rh12,rh8-1rh12-1, rh8-1rh6-1* and *rh6-1rh-12-1*14-days-old seedlings by RT-qPCR. The expression was normalized to ubiquitin mRNA and expressed relative to Col-0. Values represent a

For Peer Review

mean of three independent biological replicates with standard error of the mean (SEM) shown by error bars, *P < 0.05, **P < 0.01, ***P < 0.001 (t-test).

Fig.3 Localization and co-localization of the RH12 and RH14 with UPF proteins in Arabidopsis protoplasts.

(A) Localization of UPF1-YFP and UPF3-YFP fusion proteins in Arabidopsis mesophyll protoplasts (left, yellow panels). Overlay and red fluorescence of chloroplasts (right). (B) Localization of RH12-CFP (DDX6) (left, cyan, upper panel). Co-localization of RH12-CFP with UPF1-YFP (middle panel) or with UPF3-YFP (lower panel). (C) Localization of RH14-CFP (DDX5) (left, cyan, upper panel). Co-localization of RH14-CFP with UPF1-YFP (middle panel) or with UPF3-YFP (lower panel). Nucleus is marked by yellow arrows, nucleolus by red arrows and P-bodies by green arrows. Scale bars represent 5 μm.

Fig.4 Localization and co-localization of RH11 with UPFs proteins in *N. benthamiana* leaves.

Localization of RH11-CFP (DDX3) (left, cyan upper panel). Co-localization of DDX3-CFP with UPF1-YFP (middle panel) and with UPF3-YFP (lower panel). Nucleus is marked by yellow arrows, nucleolus by red arrows and P-bodies are green. Scale bars represent 5 μm.

Supplementary data

Supplementary data are available at PCP online.

Methods S1. Additional methods.

Supplementary Table S1. List of proteins identified in UPF1 immunoprecipitations.

A list of all proteins, which were identified in at least two out of three UPF1 co-IP samples or enriched compared to negative samples. Proteins identified exclusively in UPF1 co-IP (not found in Col-0) are marked in blue. Columns D-F, three control IP replicas from Col-0 plants; columns G-I, three control IP replicas from UPF1-SF plants; columns J-O, normalized values of identified peptides (number of queries) in control (columns J-L) or UPF1 co-IP (M-O) samples; column P, enrichment estimate value (differences in median normalized number of queries between UPF1 co-IP and control samples).

Supplementary Table S2. Common UPF1 interactors identified in 14-days-old seedlings (our work) and flowers (Chicois et al. 2018).

Supplementary Table S3. Comparison of *A. thaliana* DDX3, DDX6, DDX5 helicases.

Supplementary Table S4. Comparison of *A. thaliana* and *N. benthamiana* DDX3, DDX6, DDX5 helicases.

Supplementary Table S5. List of primers.

For Peer Review

Figure 1

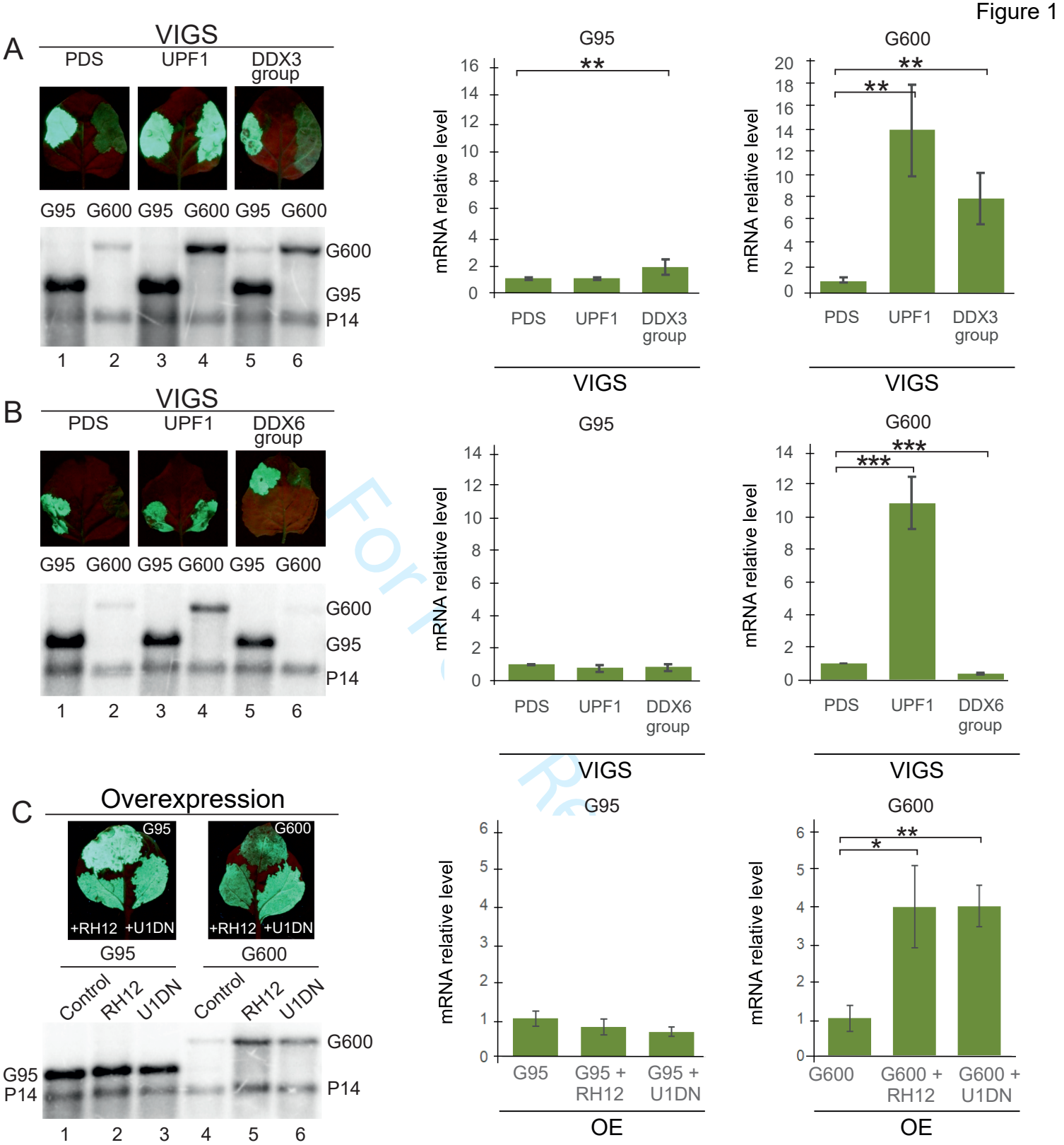
A
VIGS
PDS
UPF1
DDX3 group
G95 G600 G95 G600 G95 G600
G600
G95
P14
1 2 3 4 5 6
B
VIGS
PDS
UPF1
DDX6 group
G95 G600 G95 G600 G95 G600
G600
G95
P14
1 2 3 4 5 6
C
Overexpression
G95
G600
+RH12 +U1DN
+RH12 +U1DN
G95
G600
Control RH12 U1DN Control RH12 U1DN
G600
G95
P14
P14
1 2 3 4 5 6
G95
mRNA relative level
PDS UPF1 DDX3 group
VIGS
G600
mRNA relative level
PDS UPF1 DDX3 group
VIGS
G95
mRNA relative level
PDS UPF1 DDX6 group
VIGS
G600
mRNA relative level
PDS UPF1 DDX6 group
VIGS
G95
mRNA relative level
G95 G95 + RH12 G95 + U1DN
OE
G600
mRNA relative level
G600 G600 + RH12 G600 + U1DN
OE

Figure 2

A

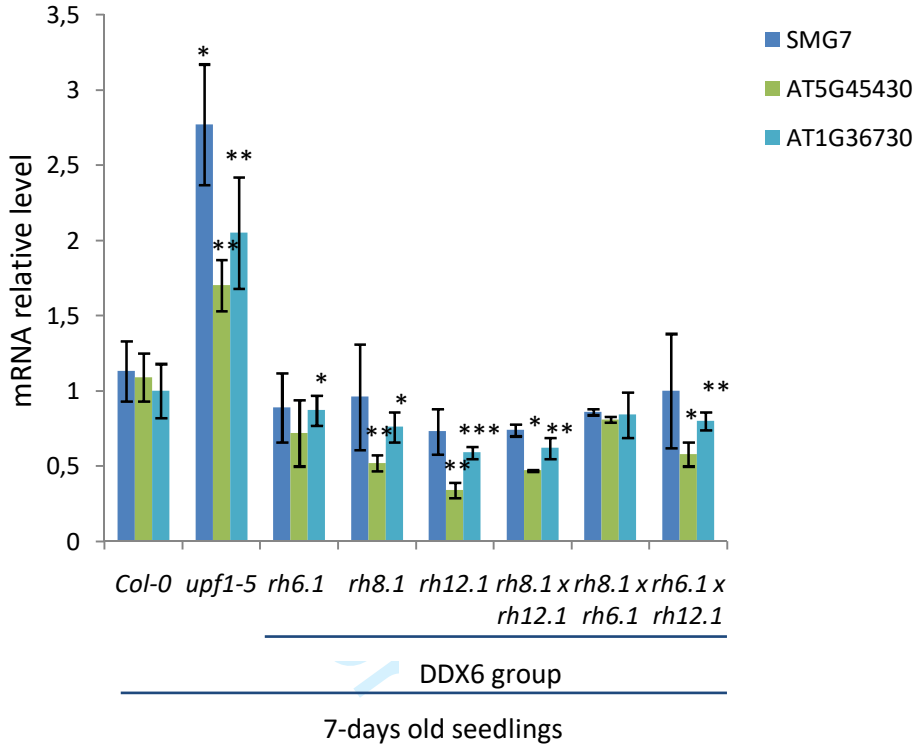
3,5
3
2,5
2
1,5
1
0,5
0
mRNA relative level
SMG7
AT5G45430
AT1G36730
Col-0
upf1-5
rh6.1
rh8.1
rh12.1
rh8.1 x rh12.1
rh8.1 x rh6.1
rh6.1 x rh12.1
DDX6 group
7-days old seedlings

B

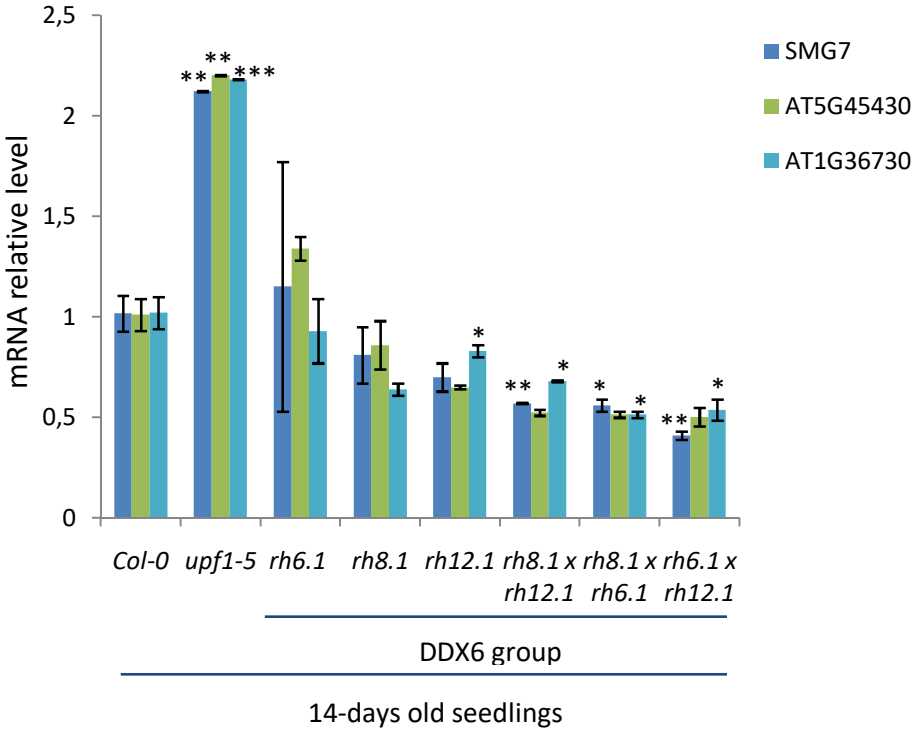
2,5
2
1,5
1
0,5
0
mRNA relative level
SMG7
AT5G45430
AT1G36730
Col-0
upf1-5
rh6.1
rh8.1
rh12.1
rh8.1 x rh12.1
rh8.1 x rh6.1
rh6.1 x rh12.1
DDX6 group
14-days old seedlings

Figure 3

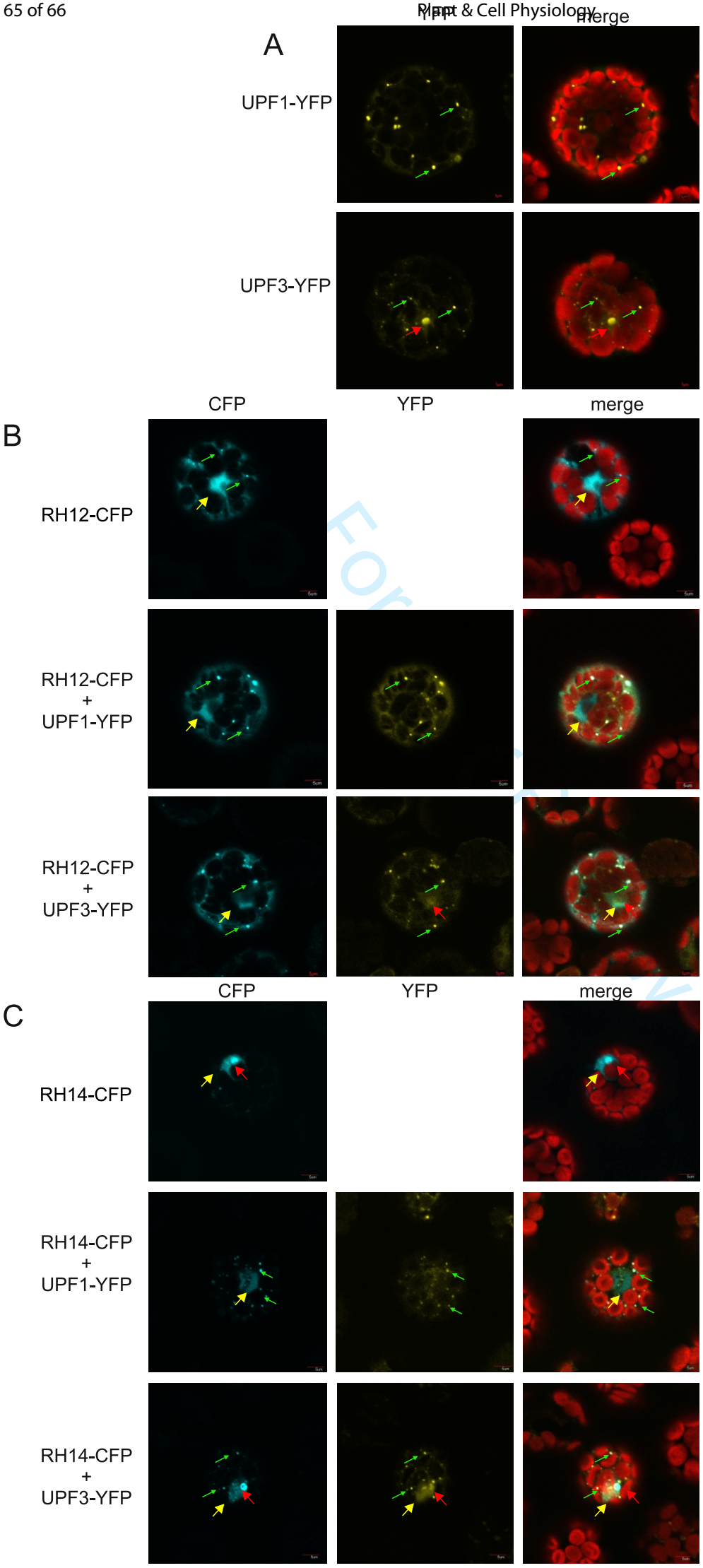
A
YFP
merge
UPF1-YFP
UPF3-YFP
B
CFP
YFP
merge
RH12-CFP
RH12-CFP + UPF1-YFP
RH12-CFP + UPF3-YFP
C
CFP
YFP
merge
RH14-CFP
RH14-CFP + UPF1-YFP
RH14-CFP + UPF3-YFP

Figure 4

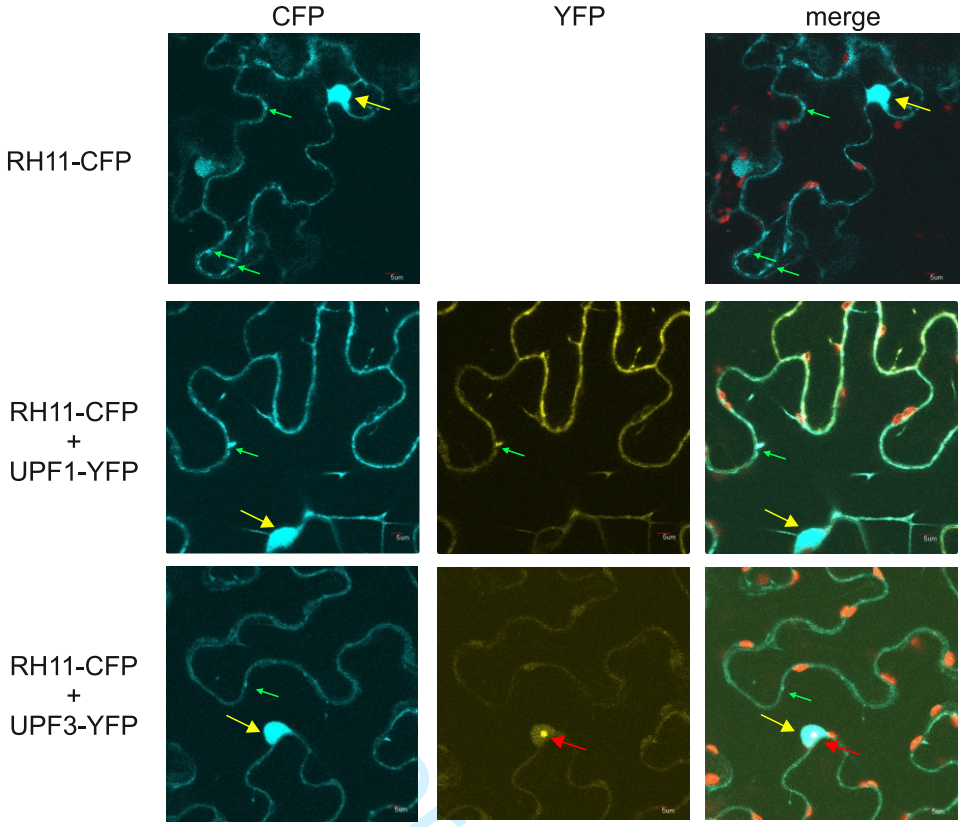

For Peer Review

Figure S1

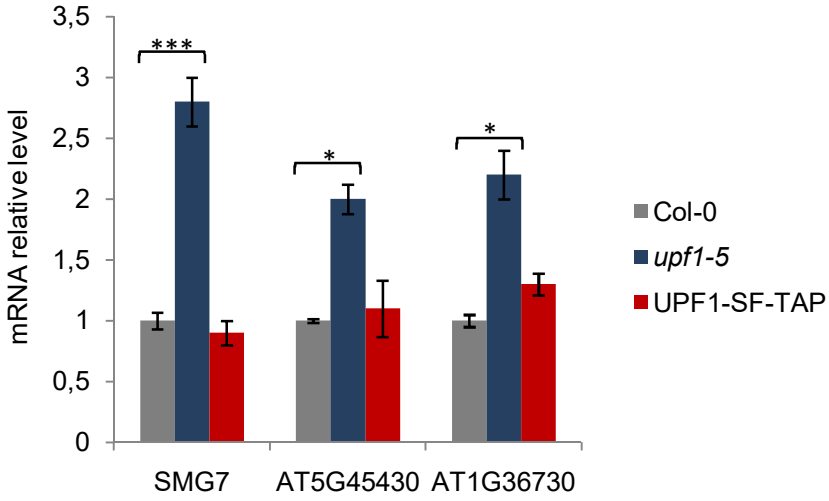
3,5
3
2,5
2
1,5
1
0,5
0
mRNA relative level
***
*
*
SMG7
AT5G45430
AT1G36730
Col-0
upf1-5
UPF1-SF-TAP

A

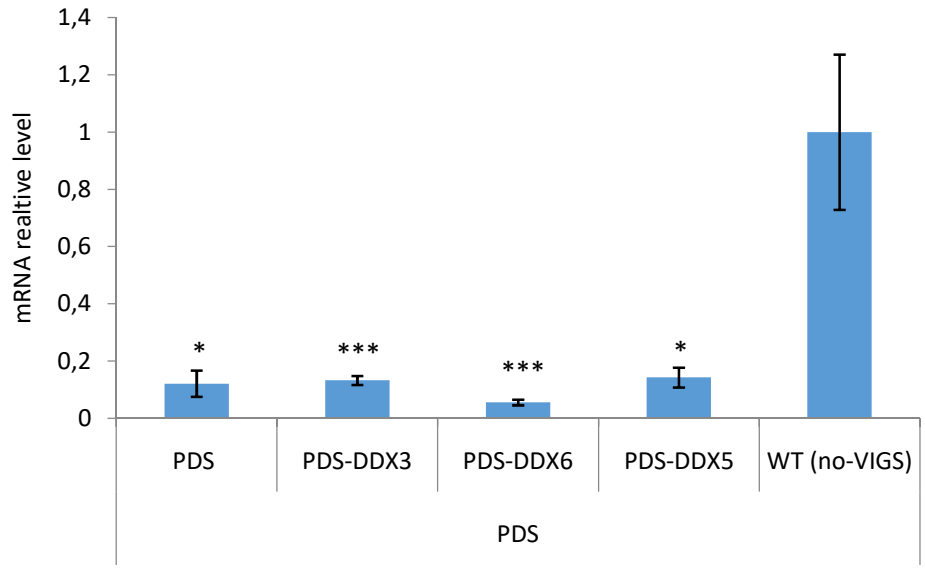
mRNA realtive level
1,4
1,2
1
0,8
0,6
0,4
0,2
0
*
***
***
*
PDS
PDS-DDX3
PDS-DDX6
PDS-DDX5
WT (no-VIGS)
PDS

B

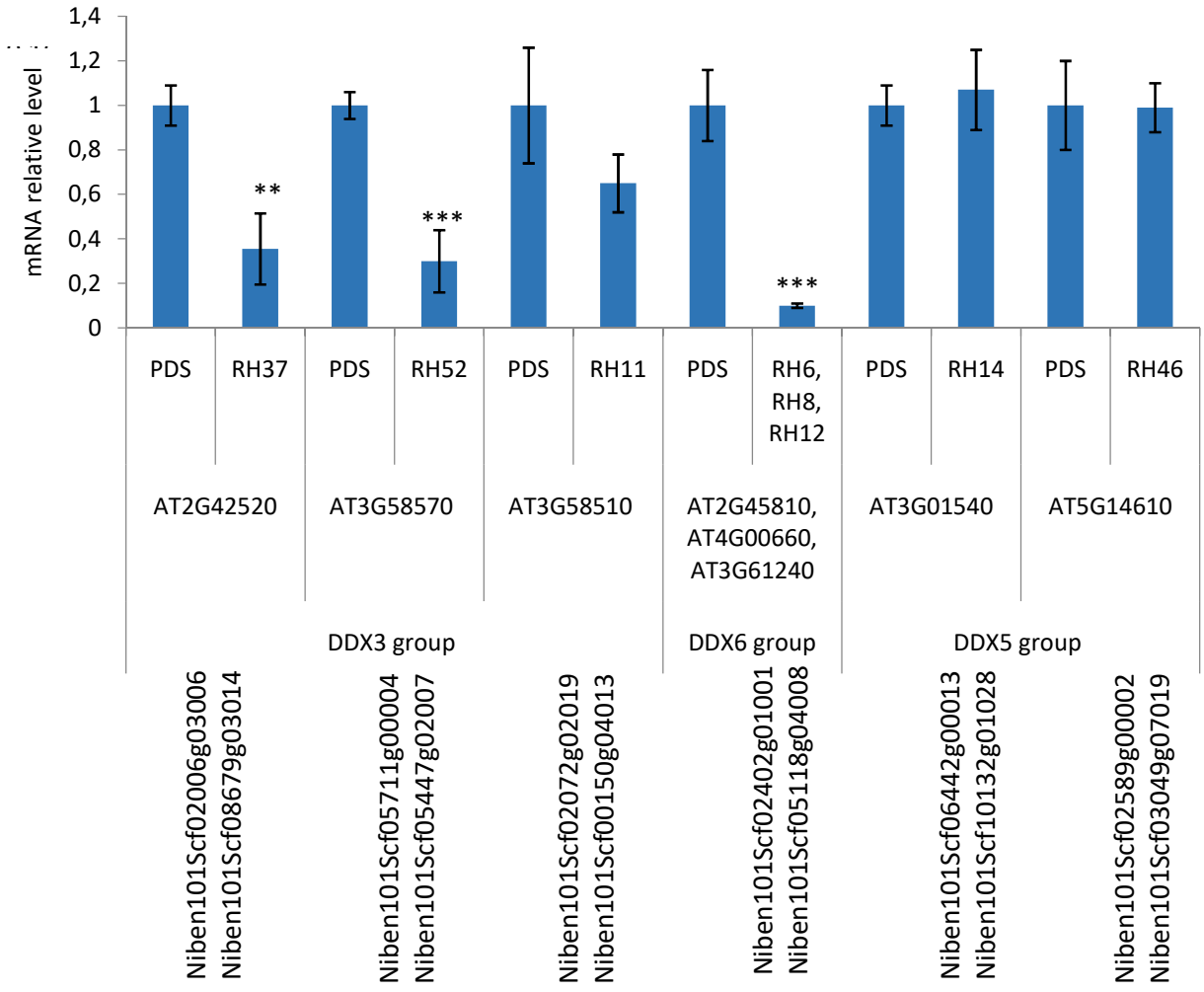
mRNA relative level
1,4
1,2
1
0,8
0,6
0,4
0,2
0
**
***
***
PDS
RH37
PDS
RH52
PDS
RH11
PDS
RH6, RH8, RH12
PDS
RH14
PDS
RH46
AT2G42520
AT3G58570
AT3G58510
AT2G45810, AT4G00660, AT3G61240
AT3G01540
AT5G14610
DDX3 group
DDX6 group
DDX5 group
Niben101Scf02006g03006
Niben101Scf08679g03014
Niben101Scf05711g00004
Niben101Scf05447g02007
Niben101Scf02072g02019
Niben101Scf00150g04013
Niben101Scf02402g01001
Niben101Scf05118g04008
Niben101Scf06442g00013
Niben101Scf10132g01028
Niben101Scf02589g00002
Niben101Scf03049g07019

B

A

Sequence alignment of the DDX3 group

Figure S3

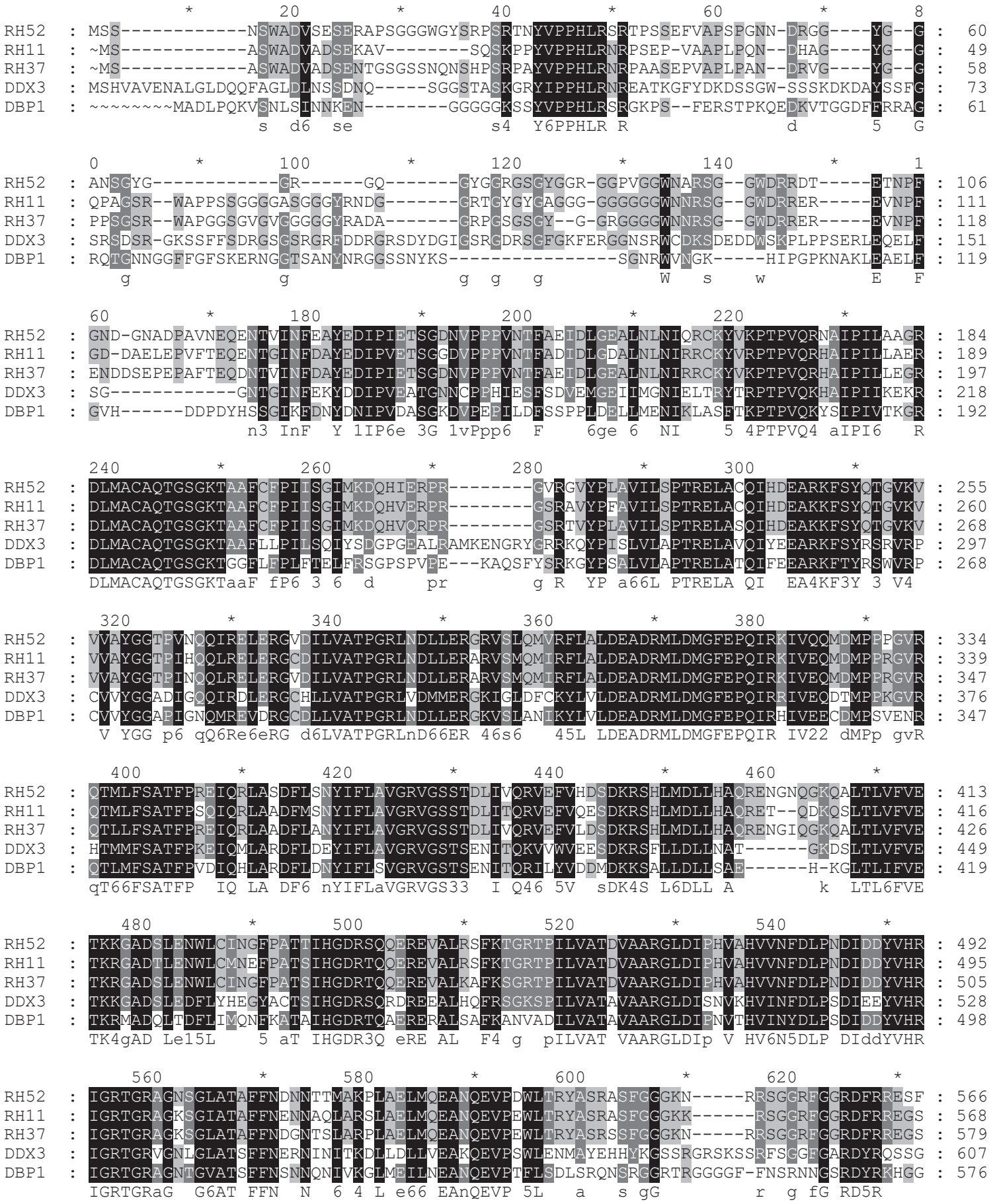

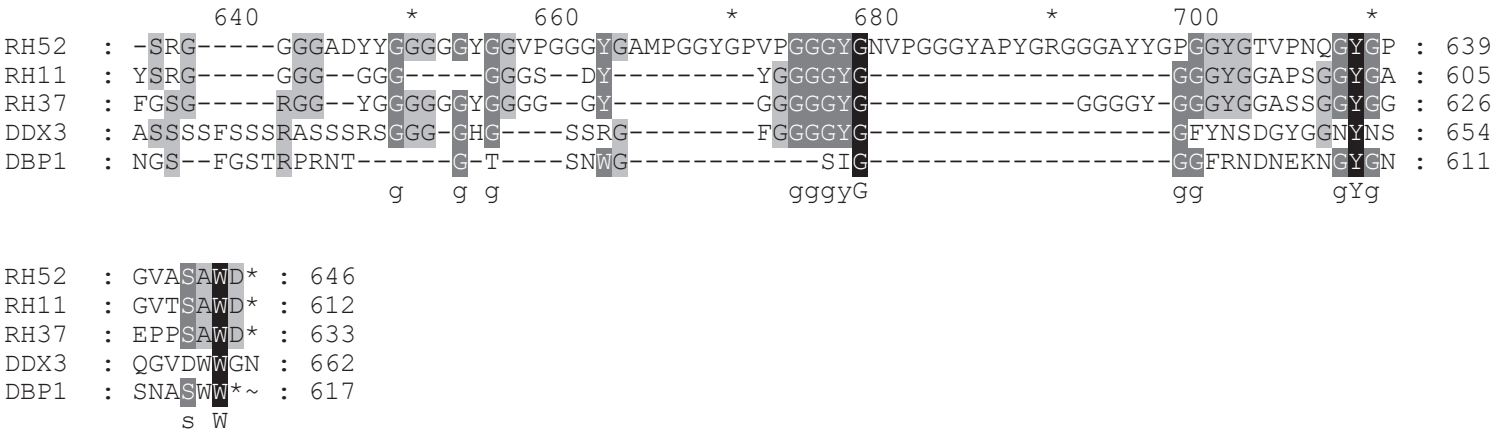
640 * 660 * 680 * 700 *
RH52 : -SRG-----GGGADYYGGGGGYGGVPGGGYGAMPGGYGPVPGGGYGNVPGGGYAPYGRGGGAYYGPGGYGTVPNQGYGP : 639
RH11 : YSRG-----GGG--GGG-----GGGS--DY---------YGGGGYG-------------------GGGYGGAPSGGYGA : 605
RH37 : FGSG-----RGG--YGGGGGGYGGGG--GY---------GGGGGYG-------------GGGGY-GGGYGGASSGGYGG : 626
DDX3 : ASSSSFSSSRASSSRSGGG-GHG----SSRG--------FGGGGYG-------------------GFYNSDGYGGNYNS : 654
DBP1 : NGS--FGSTRPRNT------G-T----SNWG------------SIG-------------------GGFRNDNEKNGYGN : 611
g g g gggyG gg gYg
RH52 : GVASAWD* : 646
RH11 : GVTSAWD* : 612
RH37 : EPPSAWD* : 633
DDX3 : QGVDWWGN : 662
DBP1 : SNASWW*~ : 617
s W

B

Sequence alignment of the DDX5 group

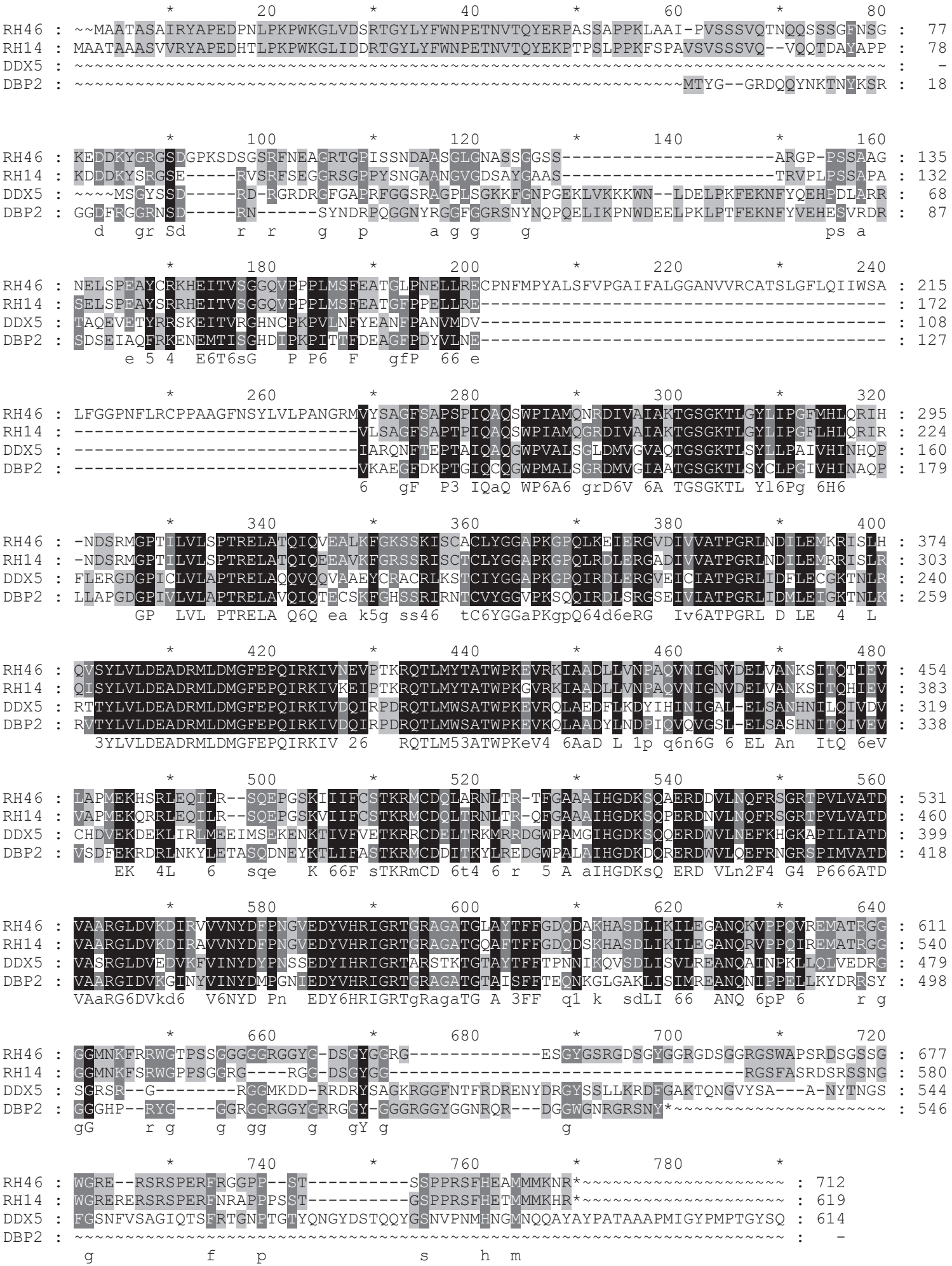

C

Sequence alignment of the DDX6 group

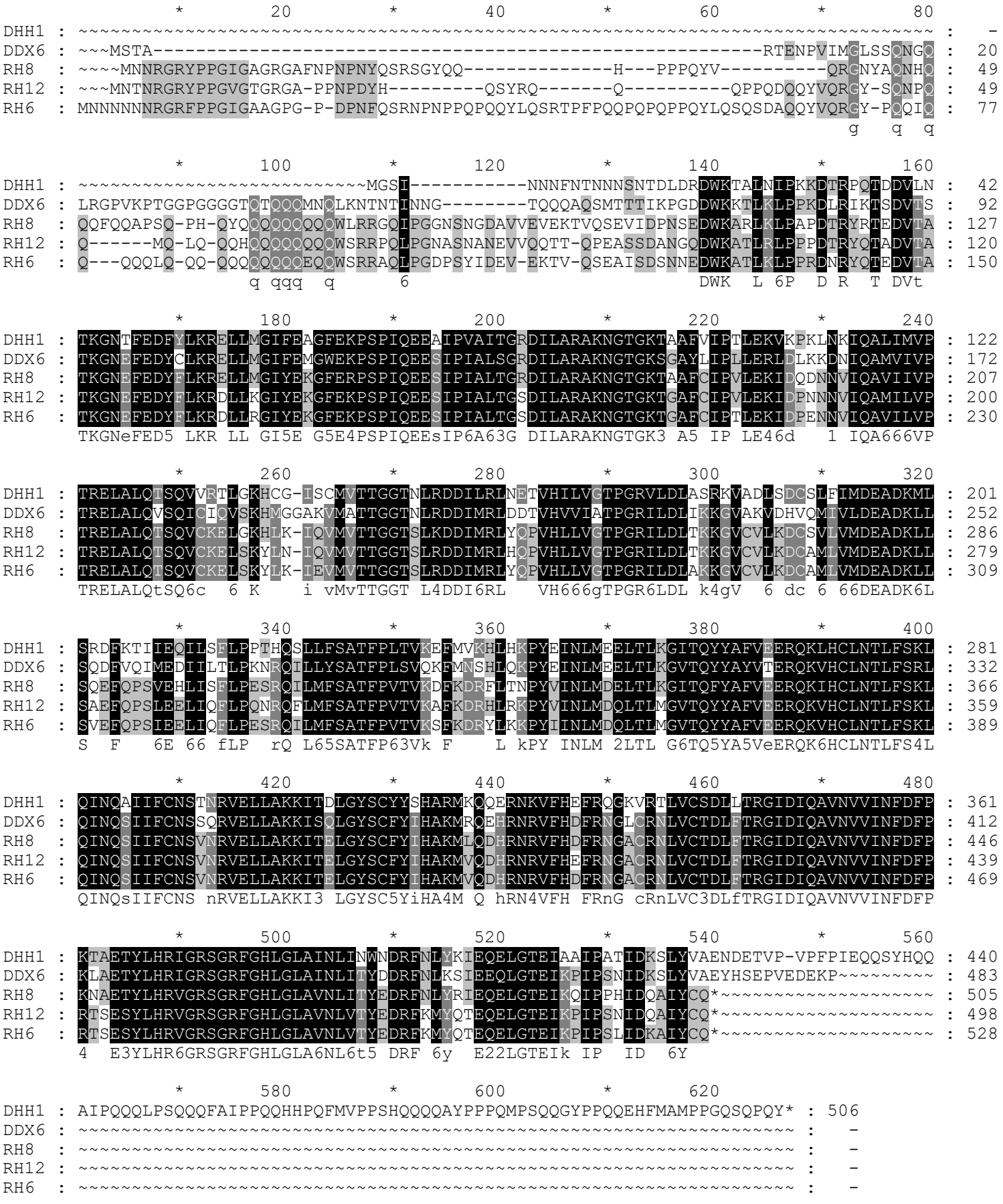

A

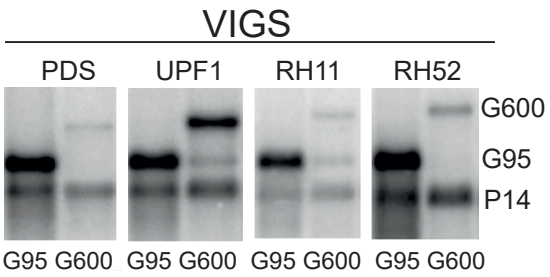
VIGS
PDS
UPF1
RH11
RH52
G600
G95
P14
G95 G600 G95 G600 G95 G600 G95 G600

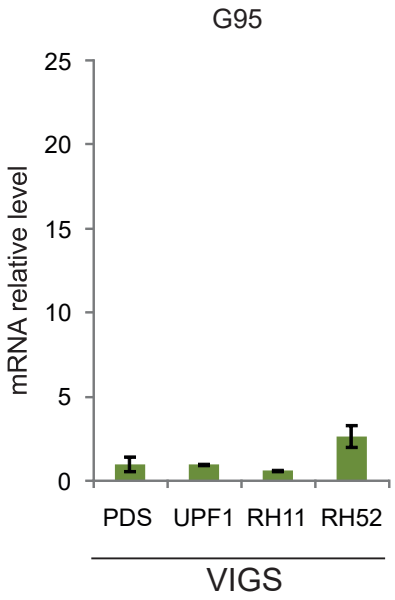
G95
mRNA relative level
25
20
15
10
5
0
PDS UPF1 RH11 RH52
VIGS

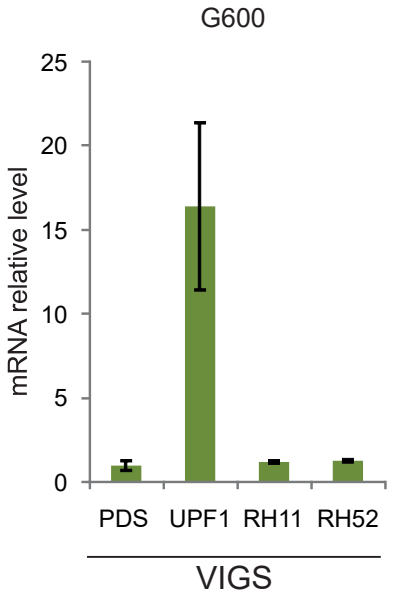
G600
mRNA relative level
25
20
15
10
5
0
PDS UPF1 RH11 RH52
VIGS

B

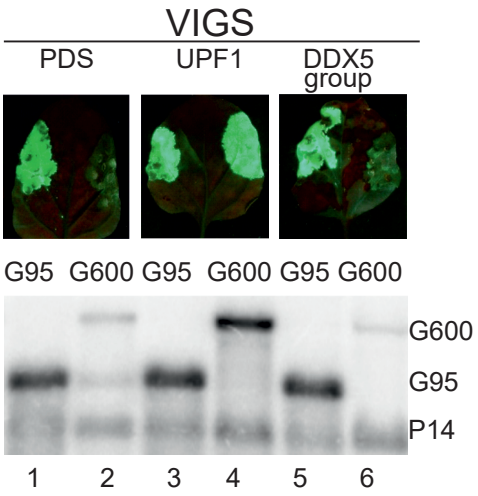
VIGS
PDS
UPF1
DDX5 group
G95 G600 G95 G600 G95 G600
G600
G95
P14
1 2 3 4 5 6

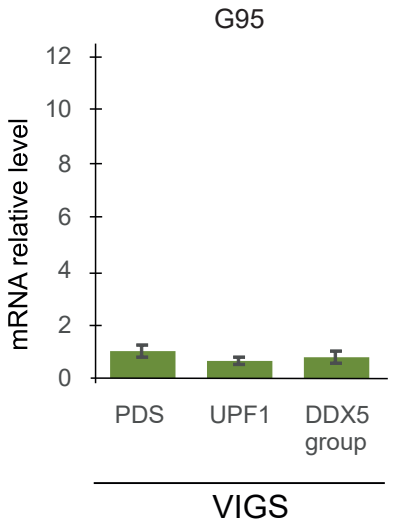
G95
mRNA relative level
12
10
8
6
4
2
0
PDS UPF1 DDX5 group
VIGS

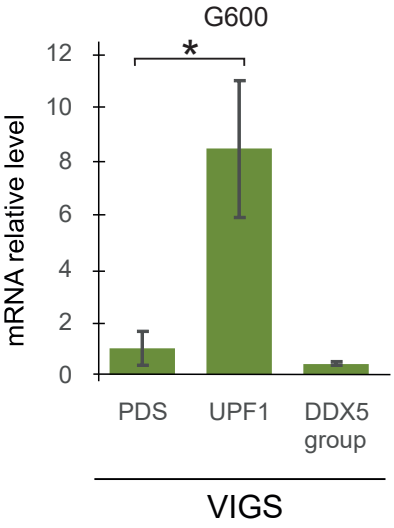
G600
*
mRNA relative level
12
10
8
6
4
2
0
PDS UPF1 DDX5 group
VIGS

Figure S5

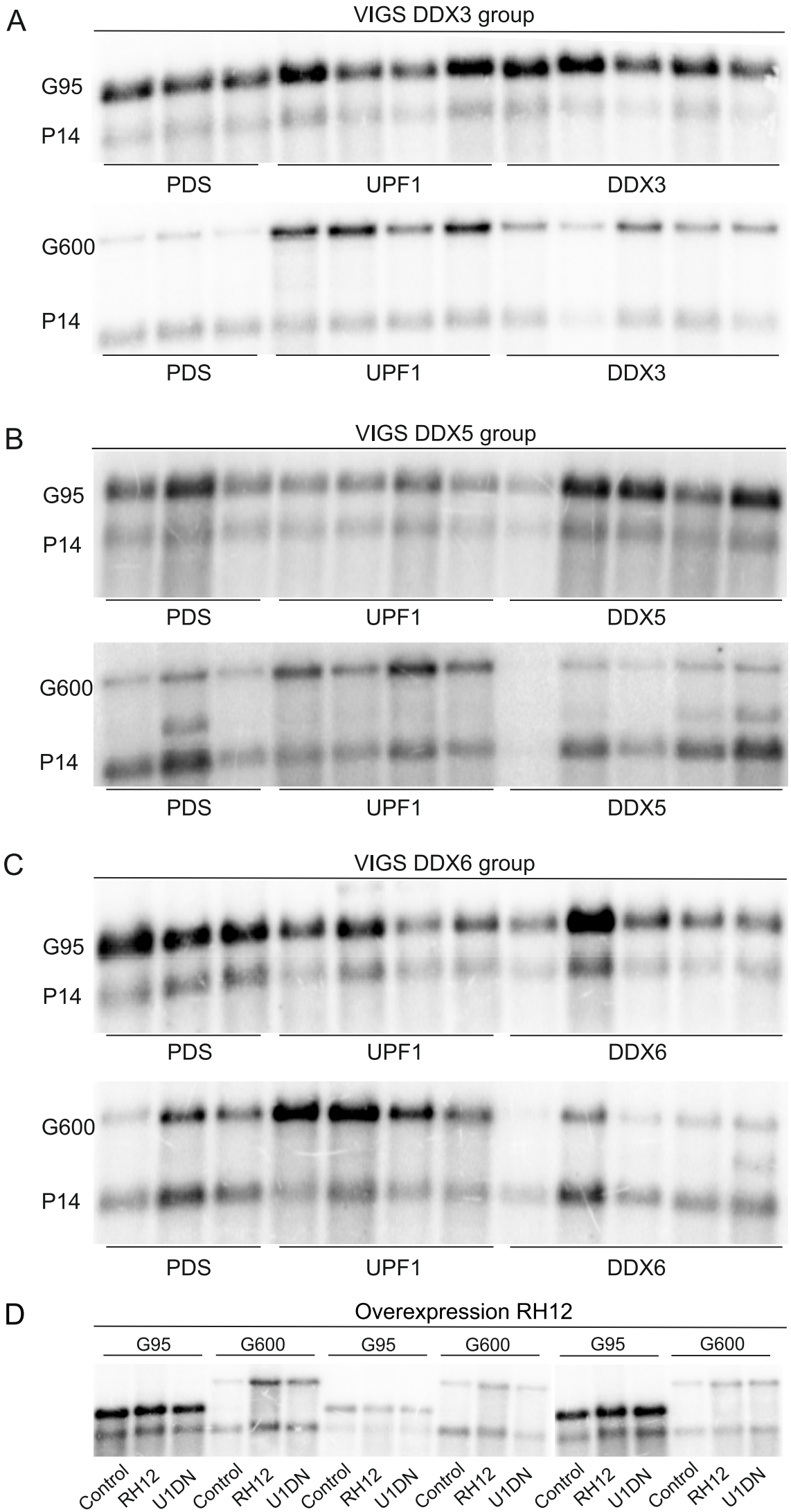
A
VIGS DDX3 group
G95
P14
PDS
UPF1
DDX3
G600
P14
PDS
UPF1
DDX3
B
VIGS DDX5 group
G95
P14
PDS
UPF1
DDX5
G600
P14
PDS
UPF1
DDX5
C
VIGS DDX6 group
G95
P14
PDS
UPF1
DDX6
G600
P14
PDS
UPF1
DDX6
D
Overexpression RH12
G95
G600
G95
G600
G95
G600
Control
RH12
U1DN
Control
RH12
U1DN
Control
RH12
U1DN
Control
RH12
U1DN
Control
RH12
U1DN
Control
RH12
U1DN

A

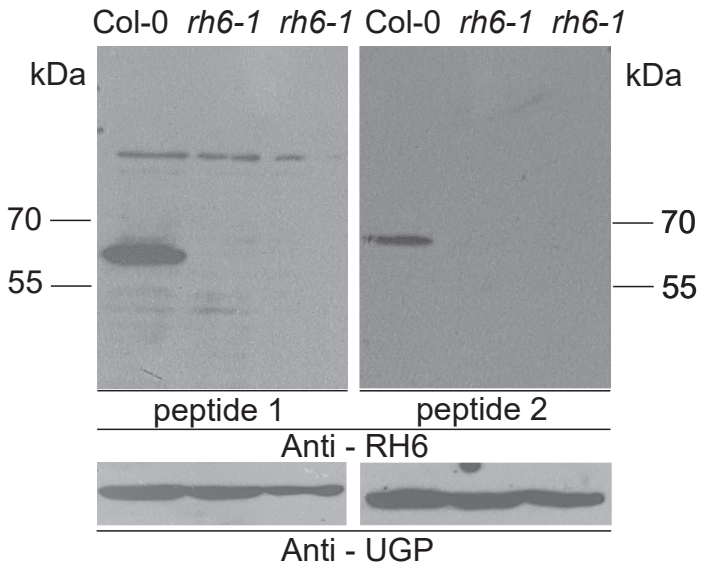
Col-0 rh6-1 rh6-1 Col-0 rh6-1 rh6-1
kDa
kDa
70
55
70
55
peptide 1
peptide 2
Anti - RH6
Anti - UGP

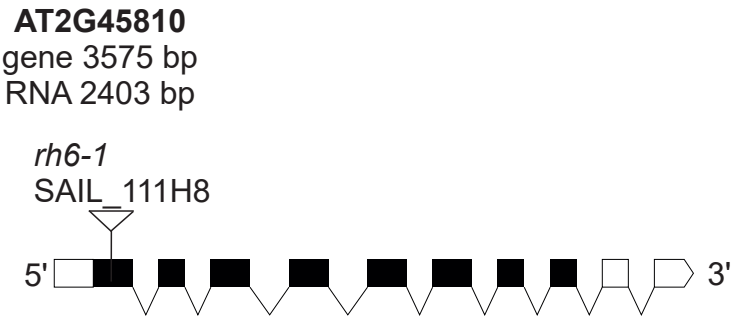
AT2G45810
gene 3575 bp
RNA 2403 bp
rh6-1
SAIL_111H8
5'
3'

B

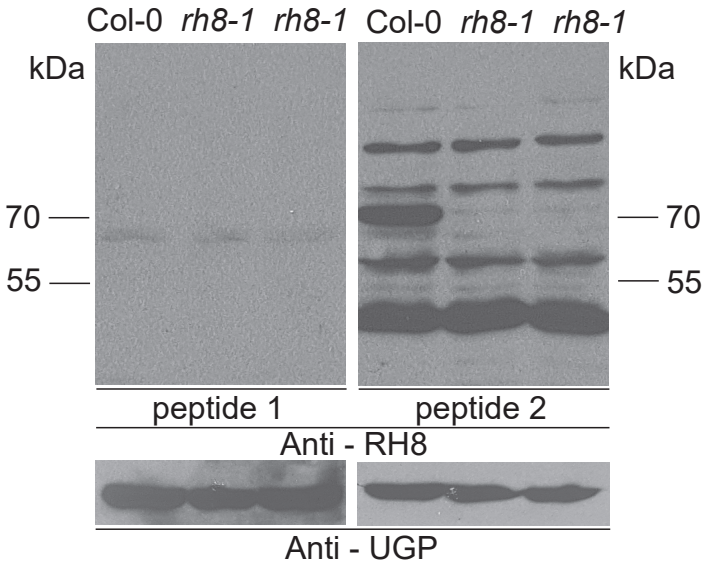
Col-0 rh8-1 rh8-1 Col-0 rh8-1 rh8-1
kDa
kDa
70
55
70
55
peptide 1
peptide 2
Anti - RH8
Anti - UGP

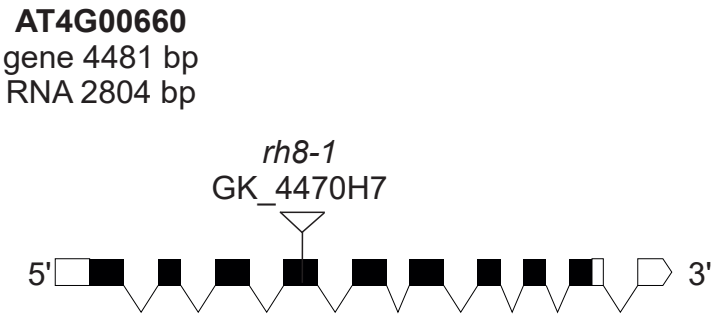
AT4G00660
gene 4481 bp
RNA 2804 bp
rh8-1
GK_4470H7
5'
3'

C

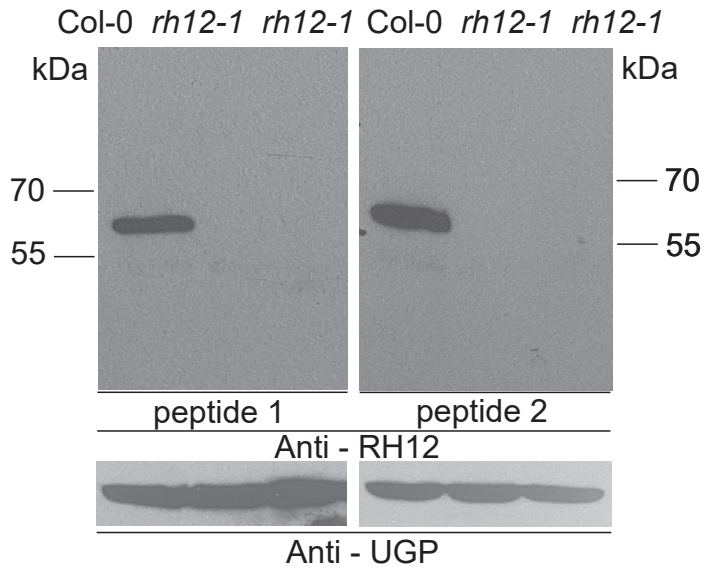
Col-0 rh12-1 rh12-1 Col-0 rh12-1 rh12-1
kDa
kDa
70
55
70
55
peptide 1
peptide 2
Anti - RH12
Anti - UGP

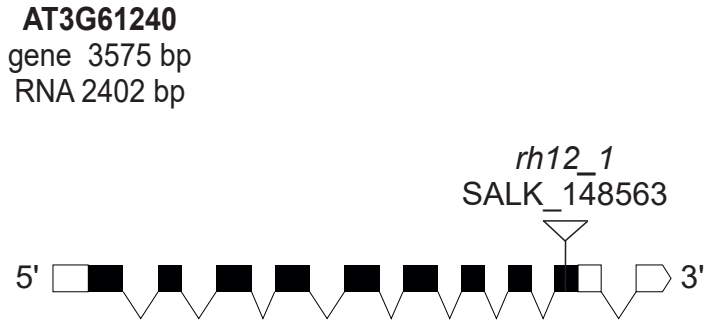
AT3G61240
gene 3575 bp
RNA 2402 bp
rh12_1
SALK_148563
5'
3'

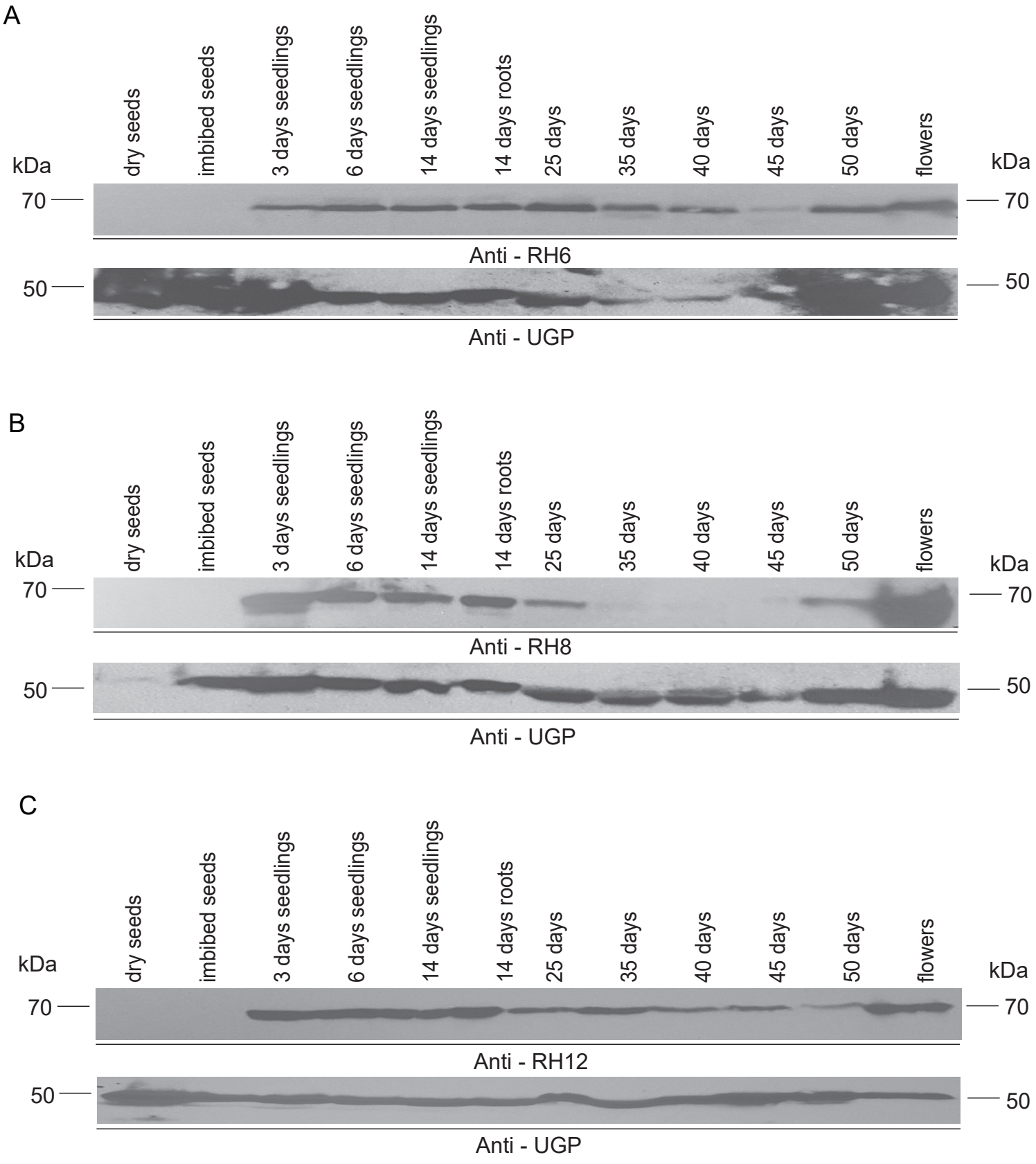
A
dry seeds
imbibed seeds
3 days seedlings
6 days seedlings
14 days seedlings
14 days roots
25 days
35 days
40 days
45 days
50 days
flowers
kDa
70
50
Anti - RH6
Anti - UGP
B
Anti - RH8
Anti - UGP
C
Anti - RH12
Anti - UGP

Figure S8

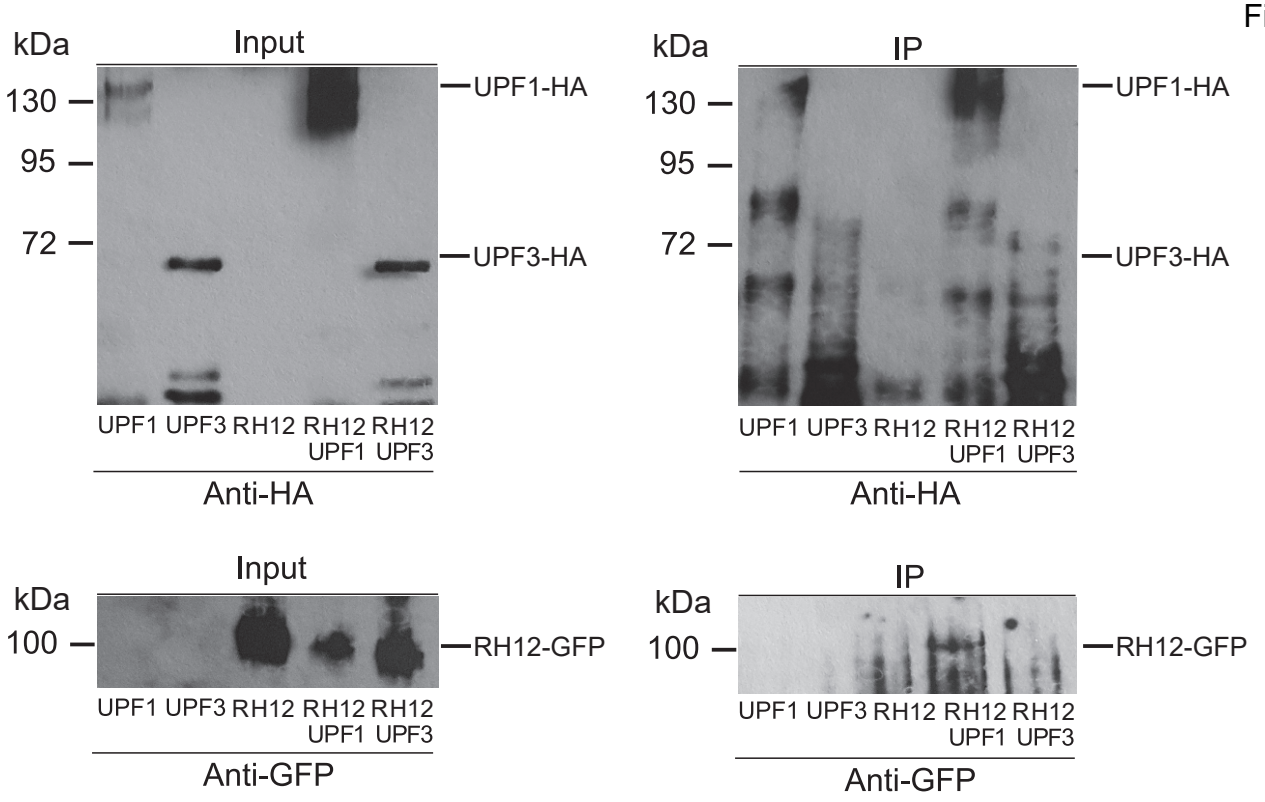
kDa
Input
130
95
72
UPF1-HA
UPF3-HA
UPF1 UPF3 RH12 RH12 RH12
UPF1 UPF3
Anti-HA
kDa
IP
130
95
72
UPF1-HA
UPF3-HA
UPF1 UPF3 RH12 RH12 RH12
UPF1 UPF3
Anti-HA
Input
kDa
100
RH12-GFP
UPF1 UPF3 RH12 RH12 RH12
UPF1 UPF3
Anti-GFP
IP
kDa
100
RH12-GFP
UPF1 UPF3 RH12 RH12 RH12
UPF1 UPF3
Anti-GFP

Figure S9

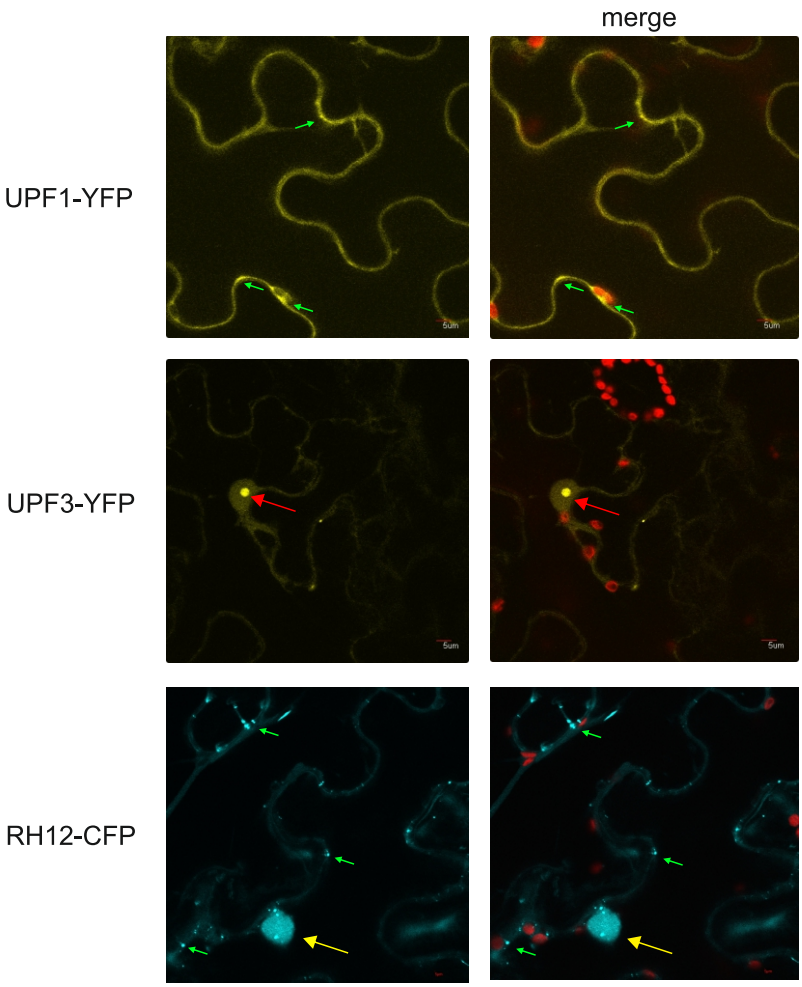

Common UPF1 interactors		
1	AT5G47010	**UPF1**
2	AT2G39260	**UPF2**
3	AT1G33980	**UPF3**
4	AT2G45810	RH6
5	AT4G00660	RH8
6	AT3G61240	RH12
7	AT3G58510	RH11
8	AT2G42520	RH37
9	AT3G58570	RH52
10	AT3G01540	RH14
11	AT5G14610	RH46
12	AT1G54270	eIF4A-2
13	AT3G13920	eIF4A (RH4)
14	AT4G34110	PAB2
15	AT2G23350	PAB4
16	AT1G49760	PAB8
17	AT1G22760	PAB3

Table S3. Comparison of A. thaliana DDX3, DDX5, DDX6 helicases.

A

	DDX3 group		
	RH11	**RH37**	**RH52**
RH11	x	85%	71%
RH37	85%	x	82%
RH52	71%	82%	x

B

	DDX6 group		
	RH12	**RH8**	**RH6**
RH12	x	80%	80%
RH8	80%	x	77%
RH6	80%	77%	x

C

	DDX5 group	
	RH14	**RH46**
RH14	x	78%
RH46	78%	x

Table S4. Comparsion of A. thaliana and N. benthamiana DDX3, DDX5, DDX6 helicases.

Name	*A. thaliana* accession numbers	*N. benthamiana* accession numbers	Niben101Scf02006g03006 fragment similarity	Niben101Scf05711g00004 fragment similarity
DDX3 group	AT2G42520	Niben101Scf02006g03006	**100,00%**	**82,45%**
		Niben101Scf08679g03014	**99,64%**	**82,87%**
	AT3G58570	Niben101Scf05711g00004	**79,78%**	**100,00%**
		Niben101Scf05447g02007	**79,34%**	**100,00%**
	AT3G58510	Niben101Scf02072g02019	**90,74%**	**82,21%**
		Niben101Scf00150g04013	**90,45%**	**81,82%**

Name	*A. thaliana* accession numbers	*N. benthamiana* accession numbers	similarity
DDX6 group	AT2G45810	Niben101Scf02402g01001	**100,00%**
	AT4G00660	Niben101Scf05118g04008	**99,74%**

Name	*A. thaliana* accession numbers	*N. benthamiana* accession numbers	Niben101Scf06442g00013 fragment similarity	Niben101Scf08873g01020 fragment similarity	Niben101Scf33352g00001 fragment similarity
DDX5 group	AT3G01540	Niben101Scf06442g00013	**100,00%**		
		Niben101Scf10132g01028	**98,93%**		
	AT5G14610	Niben101Scf02589g00002	**86,02%**		
		Niben101Scf03049g07019	**86,02%**		
	AT3G06480	Niben101Scf04633g00010	**84,72%**		
		Niben101Scf04638g01009	**84,45%**		
		Niben101Scf08873g01020		**100,00%**	
		Niben101Scf16592g00007		**99,81%**	
	AT1G55150	Niben101Scf33352g00001			**100,00%**
		Niben101Scf15419g01004			**99,44%**
	AT5G63120	Niben101Scf01397g00012	**95,74%**		
		Niben101Scf05523g00016	**86,51%**		

Table S5. List of primers

Primer name	Sequence
Primers used to generate UPF1-STREP-FLAG tag *A. thaliana* line	
AtUPF1 promoter F	5' TATATGTACGTGTGGTTGTT 3'
AtUPF1 promoter R	5' CGTTCTAGATAGAAAAAATCAG 3'
Primers used to generate constructs for VIGS-NMD	
Nb DHH1 VIGS EI F	5' cataGAATTCCCGGAGTTCCAACCTTCCATTGTGC 3'
Nb DHH1 VIGS EI R	5' cataGAATTCGCGGAAGTCATGAAACACTCTGTTCC 3'
Nb DDX3X VIGS EI F	5' cataGAATTCAGACTAGCCTCGGATTTTCTATCCAG 3'
Nb DDX3X VIGS OL R	5'ATAAGAGCAAGGGGAAACACTGTCCGAATTGTTCTCATTGAAGA AGGCAGTAGC 3'
Nb DDX3X VIGS OL F	5'GCTACTGCCTTCTTCAATGAGAACAATTCGGACAGTGTTTCCCC TTGCTCTTAT 3'
Nb DDX3X VIGS EI R	5' cataGAATTCGTACTCGAACCAACCCGTCCAACTGC 3'
Nb DBP2 VIGS EI F	5' cataGAATTCAGATCTTGAGATCCCAAGAACCAGG 3'
Nb DBP2 VIGS OL1 R	5'CCGAGAATATATATGAGGTGGACCCACTGAAGCATGCTTAGCAT CCTGG 3'
Nb DBP2 VIGS OL 1 F	5'CCAGGATGCTAAGCATGCTTCAGTGGGTCCACCTCATATATATT CTCGG 3'
Nb DBP2 VIGS OL 2 R	5'GGATTTGAGGTTCAAAACCCATGTCCTTTTCGAAGGGTACCAAG TTTCC 3'
Nb DBP2 VIGS OL 2 F	5'GGAAACTTGGTACCCTTCGAAAAGGACATGGGTTTTGAACCTCA AATCC 3'
Nb DBP2 VIGS long EI R	5' cataGAATTCTCACCATGAATAGAAAGTGCAGGCC 3'
Primers for RT-qPCR	
qUBC9 R	5' ACTCCTCCAGAATAAGGGCTATCCG 3'
qUBC9 F	5' TTCATGTAGCGCAGGACCCGTTG 3'
qAT5G45430 R	5' CCTTCCCGGTGGTCTATACTTTG 3'
qAT5G45430 F	5' GACCCAGCAGAAGGTGGATAC 3'
qAT1G36730 R	5' AGTTGGGTAGGAGATGAACCAC 3'
qAT1G36730 F	5' GTGAAGAAGGCACCAGAACAAG 3'
qSMG7 R	5' CAAGAAGCCAAGGCCACAAAG 3'
qSMG7 F	5' TGGGAATGATGCAGGTGAGTG 3'
qNiben101Scf02006g03006 Niben101Scf08679g03014 F	5' CCTCTTACAATCGAGGCGCTG 3'
qNiben101Scf02006g03006 Niben101Scf08679g03014 R	5' TGCACTAGTCACACCTGCTGC 3'
qNiben101Scf05711g00004 Niben101Scf05447g02007 F	5' GGGCGTGACTTCAGGAGGG 3'
qNiben101Scf05711g00004 Niben101Scf05447g02007 R	5' CCAGGACCATATCCCCCGC 3'

qNiben101Scf02072g02019 Niben101Scf00150g04013 F	5' CCACCCACATTTTGCCCCAC 3'
qNiben101Scf02072g02019 Niben101Scf00150g04013 R	5' ACCACCATTGCAGCGAAGAC 3'
qNiben101Scf02402g01001 Niben101Scf05118g04008 F	5' ACTGCTGCTTTCTGCATTCCG 3'
qNiben101Scf02402g01001 Niben101Scf05118g04008 R	5' GCCAATTCTCGTGTGGGAACAA 3'
qNiben101Scf06442g00013 Niben101Scf10132g01028 F	5' GGTCATGGCTCTCGTGATACCG 3'
qNiben101Scf06442g00013 Niben101Scf10132g01028 R	5' GGGCTTCTGCTCCGACTTCG 3'
qNiben101Scf02589g00002 Niben101Scf03049g07019 F	5' CTCCGCCTCAGCAACCCAAG 3'
qNiben101Scf02589g00002 Niben101Scf03049g07019 R	5' CCCACTAGGAAGAACCGGTGC 3'
Primers to clone DDX helicases	
pENTR RH11 R	5' TACAAG AAAGCT GGGTCT AGATAT CTATCC CAAGCA CTGGTC ACTCC 3'
pENTR RH11 F	5' CAATTC AGTCGA CTGGAT CCGGTA CATGAG TGCATC ATGGGC AGATG 3'
pENTR RH12 R	5' GAAAGC TGGGTC TAGATA TCTCTG ACAGTA GATTGC TTGATC 3'
pENTR RH12 F	5' CAGTCG ACTGGA TCCGGT ACATGA ATACTA ACAGAG GAAGAT ATC 3'
pENTR RH14 R	5' TACAAG AAAGCT GGGTCT AGATAT CTTCTG TGTTTC ATCATC ATCGTC TCG 3'
pENTR RH14 F	5' CAATTC AGTCGA CTGGAT CCGGTA CATGGC TGCTAC CGCTGC TGC 3'
Primers for genotyping Arabidopsis T-DNA insertion plants	
RH6 LP-SAIL111H08	5’ TCCAACCAGTAAATGGACAGG 3’
RH6 RP-SAIL111H08	5’ ATAGAGGAAGATTTCCACCGG 3’
RH8 LP-GK447H07	5’ ATGGAACACTCTGTTTCGGTG 3’
RH8 RP-GK447H07	5’ CAAAGCTGGCGTCGTAAATAG 3’
RH12 LP-SALK148563	5’ CTAGGGAGAGATCTCCACAGG 3’
RH12 RP-SALK148563	5’ TCGAGGAATTGACATTCAAGC 3’

Supplementary Figure Legends

Supplementary Fig. S1Complementation of the *upf 1-5* line with UPF1-SF.

mRNA level of *SMG7*, *AT5G45430* and *AT1G36730* NMD endogenous substrates in Col-0, *upf1-5,* and *upf1-5* complemented with UPF1-STREP-FLAG (UPF1-SF-tag) in 14-days-old seedlings by RT-qPCR. The expression was normalized to ubiquitin mRNA and expressed relative to Col-0. Values represent a mean of three independent biological replicates with standard deviations shown by error bars (SD); *P < 0.05; ***P < 0.001 (t-test).

Supplementary Fig. S2 Silencing efficiency of DDX helicases in VIGS plants

(A) The level of *N. benthamiana PDS* mRNA in PDS-silenced, PDS-DDX3-, PDS-DDX5- and PDS-DDX6-co-silenced or WT *N. benthamiana* (non-VIGS) leaves, measured by RT-qPCR. The level of *PDS* mRNAs in PDS- and DDX/PDS-silenced plants are expressed relative to the corresponding values in the WT control arbitrarily set as 1. (B) VIGS silencing of *N. benthamiana DDX3*, *DDX5* and *DDX6* homologs (see Table S2, Supplementary Table S3, S4) in photobleached plants measured by RT-qPCR. For *DDX3* and *DDX6* all *N. benthamiana* homologs were tested, whereas for *DDX5* four *N. benthamiana* homologs, which correspond to Arabidopsis RH14 and RH46 helicases, were tested. For each DDX helicase one pair of primers recognize mRNAs of two *N. benthamiana* homologs. The level of *DDX* mRNAs in DDX-PDS-silenced plants are expressed relative to the corresponding values in PDS-silenced controls arbitrarily set as 1. Values represent a mean of at least three independent biological replicates with standard deviations (SD) shown by error bars; *P < 0.05; **P < 0.01; ***P < 0.001 (t-test). *UBC9* mRNA was used as a reference.

Supplementary Fig. S3 Sequence alignment of plant, human and yeast DDX3, DDX5 and DDX6 helicases.

Multiple sequence alignment of homologs of (A) DDX3-, (B) DDX6-, and (C) DDX5 group helicases from *Arabidopsis thaliana*: RH52, RH11, and RH37 (DDX3); RH6, RH8, and RH12 (DDX6); RH14, and RH4 (DDX5); *Homo sapiens*: DDX3; DDX6; DDX5; and *Saccharomyces cerevisiae*: Dbp1 (DDX3); Dhh1 (DDX6); Dbp2 (DDX5). Residues conserved in all homologs are highlighted in black and less conserved in grey. The alignment was created using Clustal Omega and presented using GenDoc.

Supplementary Fig. S4 NMD efficiency in single RH11- and RH52- or DDX5 group VIGS-silenced *N. benthamiana* leaves.

VIGS-NMD assay in RH11- and RH52-silenced (A) or DDX5-silenced (B) *N. benthamiana* leaves that were co-infiltrated with P14 silencing suppressor and G95 NMD-insensitive or G600 NMD-sensitive substrates. PDS-silencing (PDS) and UPF1-PDS co-silencing (UPF) were used as a negative and positive control, respectively. Northern blots (left panels) showing the mRNA level were performed using *GFP* and *P14* probes. Graphical representation (right panels) of G95 or G600 transcript level from northern blots; P14 served as a normalization control. The level of G95 or G600 in silenced leaves are expressed relative to G95 or G600 in control leaves. Values represent a mean of three independent biological replicates with standard deviations shown by error bars (SD); *P < 0.05 (t-test).

Supplementary Figure S5. Contribution of DDX3, DDX5 and DDX6 helicases to plant NMD.

Uncropped northern blots of experiments shown in Fig. 2. (A-C) VIGS-NMD assay in (A) DDX3-, (B) DDX5- or (C) DDX6- silenced *N. benthamiana* leaves that were co-infiltrated with P14 silencing suppressor and G95 NMD-insensitive or G600 NMD-sensitive substrates. PDS-silencing (PDS) and UPF1-PDS co-silencing (UPF) were used as a negative and positive control, respectively. (D) The level of reporter G95 and G600 substrates in RH12-overexpressing *N. benthamiana* leaves that were co-infiltrated with RH12 or U1DN constructs. Overexpression of UPF1 dominant negative form (U1DN) leads to inactivation of NMD and is used as a positive control. (A-D) RNA was isolated after 3 d.p.i. and northern blot was performed using *GFP* and *P14* probes.

Supplementary Fig. S6 Expression of RH6, RH8 and RH12 in *rh6-1, rh8-1* and *rh12-1* mutants.

Western blotting of (A) RH6, (B) RH8 and (C) RH12 proteins in extracts from 14-days-old seedlings of Col-0, *rh6-1*, *rh8-1* and *rh12-1,* respectively, using specific antibodies against these helicases. For each helicase antibodies obtained from Eurogentec using two different specific peptides were used. For RH6 and RH12 both peptides recognized a specific protein of an expected size (in kDa), whereas only peptide 2 gave a specific signal for RH8. Schematic representation of *RH6*, *RH8* and *RH12* genes (on the right of the Western blot for each helicase) wascreated using http://wormweb.org/exonintron. Position of T-DNA insertion in*rh6-1, rh8-1* and *rh12-1*mutant lines is indicated with triangles. UTP-glucose-1-phosphate uridylyltransferase (UGP) was used as loading control.

Supplementary Fig. S7 Expression profile of RH6, RH8 and RH12 helicases in different developmental stages and tissues.

Western blot analyses of RH6, RH8 and RH helicases steady-state levels in protein extract from plants at indicated developmental stages and from various tissues. Specific antibodies against each helicase and UGP control were used as described for Supplementary Fig. S6.

Supplementary Fig. S8 Interaction between RH12 helicase from the DDX6 family and NMD factors, UFP1 and UFP3.

Western blot analysis of co-immunoprecipitation of RH12-GFP with UPF1-HA or UPF3-HA from 21-days-old *N. benthamiana* leaves expressing the combination of infiltrated constructs (as indicated) expressing encoding RH12-GFP, UPF1-HA and UPF3-HA. Input (left panels) and immunoprecipitaes (right panels) were separated on SDS-PAGE and proteins were detected by chemiluminescence using anti-HA peroxidase and anti-GFP peroxidase antibodies. Protein size maker (kDa) is shown on the left and detected proteins are indicated on the right of each panel.

Supplementary Figure S9. Localization and co-localization of DDX6, UPF1 and UPF3 in *N. benthamiana* leaves.

Localization of UPF1-YFP (upper panel), UPF3-YFP (middle panel) and RH12-CFP (DDX6) (lower panel); overlay and red fluorescence of chloroplasts (right panels). Nucleus is marked

by yellow arrows, nucleolus by red arrows and P-bodies by green arrows. Scale bars represent 5 μm.

Supplementary Methods S1.

Plasmid constructs

The plant binary vector pGWB604-C-SF-TAP was constructed as described (Golisz et al. 2013) using pDEST/C-SF-TAP (Gloeckner et al. 2007) and pGWB604 vectors (Nakagawa et al.2009). The *UPF1* promoter was cloned into XbaI site of the pGWB604-C-SF-TAP vector and UPF1 cDNA into SalI and EcoRV sites of the pENTR1A. These constructs were used for LR recombination reactions (Invitrogen). The plasmid containing the *UPF1* sequence with the endogenous promoter was a kind gift from John W. S. Brown (University of Dundee, UK). Plasmids with G-95 and G-600 constructs, formerly named as GFP and GFP-abc, respectively, were described in (Kertész et al. 2006). For localization in *N. benthamiana* and Arabidopsis protoplasts UPF1, UPF3, RH11 proteins were fused to protoplasts localization-optimized variants of cyan or yellow fluorescent protein (CFP or YFP). Constructs for localization were obtained by LR recombination of pGD vector (Kremers et al. 2006) with pENTR1A plasmid carrying *UPF1* or *UPF3* cDNAs (a kind gift from John W. S. Brown) or pENTR1A carrying *RH11*, *RH12* or *RH14* cDNAs lacking the STOP codon. These constructs allow for the expression of YFP/CFP-tagged proteins under the control of the constitutive 35S CaMV promoter.

VIGS-constructs were cloned into the Bin61S agroinfiltration vector or into the derivatives of Bin61S. P14, Bintra, TRV-PDS, TRV-PDS-UPF1 clones were described previously (Kertész et al. 2006; Kerényi et al. 2008; Mérai et al. 2012). *N. benthamiana* homologs of the Arabidopsis DDX3-, DDX5- and DDX6- group helicases were identified using the Solgenomic's BLASTn tool and the predicted cDNA database. Sequences for VIGS fragments were selected using the Solgenomics's VIGS tool to identify the homologous regions within similar genes. Multiple sequence alignments were created using Clustal Omega and VIGS fragment region were chosen manually (Supplementary Table S3, S4). In the case of DDX3 two VIGS fragments, derived from genes Niben101Scf02006g03006 and Niben101Scf05711g00004 were required for the sufficient silencing effect. Two VIGS fragments from Niben101Scf02402g01001 gene, three from Niben101Scf06442g00013, Niben101Scf08873g01020 and Niben101Scf33352g00001 genes and one from Niben101Scf02402g01001 gene were used for efficient silencing of *N. benthamiana* DDX3-, DDX5- and DDX6- group helicases, respectively. VIGS fragments of *DDX3*, *DDX5* and *DDX6* were generated by RT-PCR and cloned into TRV-PDS vector.

All primers used in this study are listed in Supplementary Table S5.

Affinity protein purification

UPF1-SF-TAP was purified as described (Golisz et al. 2013) with minor modifications. 30 g of 2-week-old seedlings was cross-linked two times for 10 min by vacuum infiltration with 1% formaldehyde in PBS, followed by addition of glycine to a final concentration of 80mM. Seedlings were frozen in liquid nitrogen, ground in a laboratory blender (Waring) with dry ice (10x30 s), mixed with an equal amount (w/v) of Extraction buffer (100mM Tris– HCl, pH 8.0, 150mM NaCl, 2mM EDTA, 2mM DTT, 1mM PMSF, 0.5% Triton X-100 and protease inhibitor cocktail) and sonicated on ice using 4x30 s bursts (Bioruptor). The homogenate was centrifuged at 20,000g for 40 min at 4ºC and the supernatant was centrifuged at 35,000g for 1 h at 4ºC. The supernatant was concentrated approximately four times by dialysis against PEG 20000 at 4ºC and then dialyzed for 3 h at 4ºCin Dialysis buffer (50mM Tris–HCl, pH 8.0, 150mM NaCl, 1mM EDTA, 1mM DTT, 1mM PMSF, 20% glycerol). Protein extract was supplemented with 250 mg/ml RNase A (Qiagen) and incubated for 3 h at 4ºC with slow rotation with 200ml anti-FLAG-M2 resin pre-washed in Wash buffer (50mM Tris–HCl, pH 8.0, 150mM NaCl, 1mM EDTA, 1mM DTT, 0.1% Triton X-100). The flow-through fraction was separated by centrifugation for 1 min in 4ºC at 1,000 g. Resins were washed 3-4 times with 2ml of Wash buffer and twice with TBS (50mM Tris–HCl, pH 8.0, 150mM NaCl, 1mM DTT) in polyprep chromatography columns (10 ml, BioRad). Bound proteins were eluted overnight by incubation with 250 mg/ml of the FLAG peptide in TBS at 4ºC. The eluate was concentrated to a final volume of 20 ml using SpeedVac (Christ), supplemented with 100mM ammonium bicarbonate to a final volume of 50 ml, reduced with 10mM DTT for 30 min at 56ºC and alkylated with 50mM iodoacetamide for 45 min in the dark at room temperature. The alkylating agent was eliminated using 50mM DTT.

Mass spectrometry-sample preparation

Proteins samples were analyzed by liquid chromatography coupled to the mass spectrometer in the Laboratory of Mass Spectrometry, Institute of Biochemistry and Biophysics, Polish Academy of Sciences (Warsaw, Poland). Protein solutions were subjected to a standard procedure of trypsin digestion, during which proteins were reduced with 0.5 M (5 mM f.c.) TCEP for 1 h at 60°C, blocked with 200mM MMTS (10mM f.c.) for 10 min at room temperature and digested overnight with 10 ul of 0.1 ug/ul trypsin. The resulting peptide mixtures were concentrated and desalted on a RP-C18 pre-column (Waters, Milford, MA), and further peptide separation was achieved on a nano-Ultra Performance Liquid Chromatography (UPLC) RP-C18 column

(Waters, BEH130 C18 column, 75 µm i.d., 250 mm long) using ACN gradient (0-35% ACN in 160 min) in the presence of 0.1% FA at a flow rate of 250 nl/min. The column outlet was coupled directly to the ion source of the Orbitrap Velos mass spectrometer (Thermo Electron Corp., San Jose, CA) working in the regime of data-dependent MS to MS/MS switch. A blank run ensuring absence of cross-contamination from previous samples preceded each analysis.

Mass spectrometry-proteomic analysis

The raw files were pre-processed with Mascot Distiller software (v. 2.6, MatrixScience, London, UK) and a search was performed with the Mascot Search Engine (MatrixScience, London, UK, Mascot Server 2.5) against the TAIR10 non-redundant database (35,386 sequences; 14,482,855 residues). To reduce mass errors, the peptide and fragment mass tolerance settings were established separately for individual LC-MS/MS runs after a measured mass recalibration (Malinowska *et al.,* 2012), resulting in values 8ppm for parent and 0.01Da for fragment ions. The ramaining search parameters were as follows: enzyme, Trypsin; missed cleavages, 1; fixed modifications, Methylthio (C); variable modifications, Oxidation (M); instrument, HCD.

The statistical significance of peptide identifications was estimated using a joined target/decoy database search approach. This procedure provided q-value estimates for each peptide spectrum match (PSM) in the dataset. All PSMs with *q*-values >0.01 were removed from further analysis. Proteins identified by a subset of peptides from another protein were excluded from analysis. The mass calibration and data filtering were carried out with MScan software, developed in-house (http://proteom.ibb.waw.pl/mscan/). Protein enrichment of UPF1 co-IP samples compared to negative controls from untagged Col-0 plants was calculated using number of queries for each protein in a given sample normalized to the total number of queries. A difference of median values was used as an enrichment estimate.

Western analysis

We ordered from Eurogentec (double-X immunization program) custom made antibodies generated from rabbit with two RH6 specific peptides: pep1-GPDPNFQSRNPNPPQ, pos.21-35 and pep2-WSRRAQLPGDPSYID, pos.97-111. For RH8, pep1: NPNYQSRSGYQQHPP, pos.21-35 and pep2- VQSEVIDPNSEDWK. For RH12, pep1: GAPPNPDYHQSYRQQ and pep2-SRRPQLPGNASNANE, pos. 61-81.

References

Gloeckner, C.J., Boldt, K., Schumacher, A., Roepman,R. and Ueffing, M. (2007) A novel tandem affinity purification strategy for the efficient isolation and characterisation of native protein complexes. *Proteomics*, 7:4228-4234.

Golisz, A., Sikorski, P.J., Kruszka, K. and Kufel, J. (2013) Arabidopsis thaliana LSM proteins function in mRNA splicing and degradation. *Nucleic Acids Res.* 41:6232-6249.

Kerényi, Z., Mérai, Z., Hiripi, L., Benkovics, A., Gyula, P., Lacomme, C., Barta, E., Nagy, F. and Silhavy, D. (2008) Interkingdom conservation of mechanism of nonsense-mediated mRNA decay. *EMBO J.* 27:1585-1595.

Kertész, S., Kerényi, Z., Mérai, Z., Bartos, I., Pálfy, T., Barta E. and Silhavy, D. (2006) Both introns and long 3'-UTRs operate as cis-acting elements to trigger nonsense-mediated decay in plants. *Nucleic Acids Res.* 34:6147-6157.

Kremers, G.J., Goedhart, J., van Munster, E.B. and Gadella, T.W.Jr. (2006) Cyan and yellow super fluorescent proteins with improved brightness, protein folding, and FRET Förster radius. *Biochemistry*, 45:6570-6580.

Malinowska, A., Kistowski, M., Bakun, M., Rubel, T., Tkaczyk, M., Mierzejewska, J., Dadlez, M. (2012) Diffprot-software for non-parametric statistical analysis of differential proteomics data. *J. Proteomics* 75: 4062-4073.

Mérai, Z., Benkovics, A.H., Nyikó, T., Debreczeny, M., Hiripi, L., Kerényi, Z., Kondorosi, É. and Silhavy, D. (2013) The late steps of plant nonsense-mediated mRNA decay. *Plant J.* 73:50-62.

Mi, H., Muruganujan, A., Casagrande, J.T. and Thomas, P.D. (2013) Large scale gene function analysis with the PANTHER classification system. *Nat. Protoc.* 8:1551-1566.

Nakagawa, T., Ishiguro, S. and Kimura,T. (2009) Gateway vectors for plant transformation. *Plant Biotech.* 26:275-284.

Nesvizhskii, A.I., Keller, A., Kolker, E. and Aebersold, R. (2003) A statistical model for identifying proteins by tandem mass spectrometry. *Anal. Chem*. 75:4646-4658.

Szklarczyk, D., Morris, J.H., Cook, H., Kuhn, M., Wyder, S., Simonovic, M., Santos, A., Doncheva, N.T., Roth, A., Bork, P., Jensen, L.J. and von Mering, C. (2017) The STRING database in 2017: quality-controlled protein-protein association networks, made broadly accessible. *Nucleic Acids Res.* 45:362-68.